

Design of a Data Acquisition System for a Kite Power Demonstrator

A Major Qualifying Project Report
Submitted to the Faculty
of the

WORCESTER POLYTECHNIC INSTITUTE

in partial fulfillment of the requirements for the
Degree of Bachelor of Science
In Aerospace Engineering

SUBMITTED BY:

Lauren Alex
lalex@wpi.edu

Eric DeStefano
estefano@wpi.edu

Luke Fekete
fek90@wpi.edu

Scott Gary
scgary@wpi.edu

Date: April 30th 2009

Professor David Olinger, Project Advisor

1. Abstract

The goal of this project was to design and implement a data acquisition system for a kite power system. Also, the kite power system was optimized for structural and mechanical performance. Kite power has the potential to be much more economical than other forms of wind power. In a system developed by previous MQP teams, a large wind boarding kite pulls the end of a long rocking arm which turns a generator and creates electricity. In order to determine the power output of this system, as well as any inefficiencies, four key parameters were measured: torque of the flywheel, angular velocity of the shafts, angle of inclination of the lever arm, and force of the kite on the arm. Four respective sensor instruments were purchased and configured for the system. The sensor outputs were processed using a data acquisition board that was used in conjunction with LabVIEW to record measurements. Using this data, the instantaneous power was determined. To increase power, a second power system was created to utilize both ascending and descending motions of the rocking arm. All components and subcomponents were lab tested. The results of this project give further evidence to the credibility of the kite power concept.

Certain materials are included under the fair use exemption of the U.S. Copyright Law and have been prepared according to the fair use guidelines and are restricted from further use.

2. Table of Contents

1. Abstract.....	2
2. Table of Contents.....	3
3. Table of Figures.....	5
4. Introduction	7
5. Background.....	11
6. Project Objectives.....	15
7. Design Process.....	16
7.1. Kite Power Demonstrator.....	16
7.1.1. System from 2007-2008 MQP	16
7.1.2. Redesigned System	17
7.2. Data Acquisition System.....	18
7.2.1. Key Measurements.....	18
7.2.2. Instrumentation	19
7.2.2.1. Measuring Torque	20
7.2.2.2. Measuring Kite Force	26
7.2.2.3. Measuring Rotational Speed of the Flywheel Shaft	27
7.2.2.4. Measuring Inclination	28
7.2.3. Calibration.....	29
7.3. LabVIEW	34
7.4. Structural Improvements	36
7.4.1. Oscillation Control.....	36
7.4.2. Moving the Power Train	39
7.4.3. Improving A-frame	40
7.5. Power Conversion	43
7.5.1. Second Power System.....	43
7.6. Safety Improvements.....	47
7.6.1. Protective Guards.....	47
7.6.2. Lab Safety	49
7.7. Kite Application.....	50

7.7.1.	Kite Dynamics	50
7.7.2.	Sled Kites	53
8.	Testing Methodology.....	55
9.	Results.....	57
9.1.	Lab Testing.....	57
9.2.	Field Testing.....	62
10.	Conclusions.....	63
10.1.	Overall Results.....	64
11.	Future Work.....	65
12.	Reference List	67
13.	Appendix.....	68
A.	Angle Control for the Rocking Arm	68

3. Table of Figures

Figure 1-World Wind Power Capacity (Renewable Energy Policy Network, 2009).....	8
Figure 2- Power output and wind velocity for turbine and kite of 10 m ² area (Buckley, 2008) ..	10
Figure 3 - Kite Pump System (Goela, 1983).....	12
Figure 4 – Kite Gen Schematic (Kite Gen, 2008).....	13
Figure 5 - Final Design and Equipment of 2007-2008 MQP Team (Buckley, 2008)	16
Figure 6 - Basic Measurements of Rocking Arm	19
Figure 7 - Illustration of Force on Kite.....	21
Figure 8 - Diagram of power train setup with torque meter	22
Figure 9 - Solidworks Assembly of general layout of Torque meter setup	22
Figure 10 - Solidworks model of torque meter fixture	23
Figure 11 - Initial setup of (1) Torque meter (2) Couplings (3) Flywheel and (4) Generator	23
Figure 12 - Diagram of Final Setup (direct coupling to shaft)	24
Figure 13 - Generator with added fixture for shaft-to-shaft setup	25
Figure 14 - Final Setup of Torque meter and Generator.....	25
Figure 15 - Diagram and photo of Load Cell configuration	26
Figure 16 - Tachometer setup on system	27
Figure 17 - Pickup and magnetic disc in close proximity.....	27
Figure 18 - Rieker Inclinator and Illustration of Maximum Arm Angle	28
Figure 19 - Solidworks Model of Inclinator Fixture.....	29
Figure 20 - Final Setup of Inclinator on the Rocking Arm.....	29
Figure 21 - Graph of Force per millivolt of the Load cell	31
Figure 22 - TMO-1 Amplifier for Load Cell Conditioning	32
Figure 23 - Photo of Wiring setup of DAQ and instruments	33
Figure 24 - LabVIEW Front Panel.....	34
Figure 25 - LabVIEW Block Diagram.....	35
Figure 26 - Original A-frame Structure	36
Figure 27 - Initial prototype of sliding mount for control	37
Figure 28 - Solidworks Model of Sliding Mount.....	38
Figure 29 – Solidworks Model of Sliding Mount in a) Power Position & b) De-power Position	39
Figure 30 – Initial Proximity of Gearing to the Operator	40
Figure 31 - Gearing Placement	40
Figure 32 - Wear on A-frame.....	41
Figure 33 - A-frame with added cross reinforcement.....	42
Figure 34 - Sketch of Second Power System.....	43
Figure 35 - Flatspring Assembly.....	44
Figure 36 - Photos of Second Power System.....	45
Figure 37 - Solidworks Model of Acrylic Enclosure.....	47
Figure 38 - Modified Acrylic Enclosure covering the gearing	48
Figure 39 - Acrylic Panel on Front and Rear of A-frame	48

Figure 40 - Safety rules and Setup of Foam on Arm	49
Figure 41 - Diagram of Typical KiteBoarding Kite (AirBorn Kites, 2005)	51
Figure 42 - Illustration of Power/ De-Power Mechanics (PowerKiteShop.com, 2009)	52
Figure 43 - Angle of Attack with respect to turbulent flow (NASA, 2009)	53
Figure 44 - Typical Sled Kite (Wind Power Sports, 2007).....	54
Figure 45 - Testing in Lab with all chains and foam attached to ends of arm.....	56
Figure 46 - Instrumentation Curves vs. Time; a) Rocking Arm Inclination; b) Force on Arm; c) Torque on Flywheel Shaft; d) Flywheel Shaft RPM	57
Figure 47 Comparison of Instantaneous Power at Rocking Arm Pivot and Flywheel Shaft.....	58
Figure 48 - Diagram of Angular Velocity to Gear Ratio of Drive Train	60
Figure 49 - Percent Difference Data, Expected to Actual	61
Figure 51 - Oscillation Control Shown with Plunger Clip Assembly	68
Figure 52 - Detail of rear plunger clip (Note the ramped locking system added to the sliding mount)	69
Figure 53 - Detail of Front Plunger Clip.....	69
Table 1 - Table of Arm Torque.....	21
Table 2 - Table of Drive System Torque, depending on size of flywheel used.....	21
Table 3 - Instrumentation Purchased for Data Collection	Error! Bookmark not defined.

4. Introduction

The turn of the century has brought forth a heightened awareness that the world's supply of non-renewable energy is a limited resource, and there has been an increased sense of urgency to find clean, renewable energy alternatives in order to break the global reliance on petroleum and other fossil fuels. Several studies involving comprehensive systems models have estimated that maintaining current global trends could lead to the extinction of all non-renewable sources of energy by as early as 2050 (Radzicki, 1997). Although leading world countries have been pursuing alternate energy sources for years, energy demand associated with rising world population and industrial modernization of developing countries along with the inevitable economic toll has delayed the transition from petroleum. The United States transitioned from using wood for energy to coal in the 1800's and from coal to oil in the 1900's. While these transitions were stimulated by availability and cheaper costs, the energy transition the US faces today is fuelled by decreasing availability and rising costs. Rising energy demand coupled with the decreasing supply of oil and the delay in transitioning to new sources of energy is creating a widening domestic energy gap that is only being filled by an increasing number of imports. While imports remain cheaper than implementing new energy sources, the transition will be further delayed and the gap will continue to broaden (Radzicki, 1997). The only feasible solution is to pursue cost efficient, clean energy alternatives to supplement the world's use of fossil energy until we achieve the technological and economic means to make the full transition to renewable energy.

The use of power generated by the wind is an alternative that has been used around the world for hundreds of years, but it has not yet reached its full potential. Wind power is not only a renewable energy source, but it transfers the kinetic energy produced by the natural wind directly

to electrical power without producing any harmful byproducts, such as carbon dioxide, that may be contributing to global climate change. Comprehensive studies show that the earth's atmosphere contains roughly five times the world's current energy use in all forms (Cristina L Archer). Thus, the challenge is designing and implementing efficient and cost effective means of harvesting the wind's massive energy potential.

Wind power has become a popular energy alternative in the modern world. The following figure shows a dramatic increase in the world's wind power capacity since 1990.

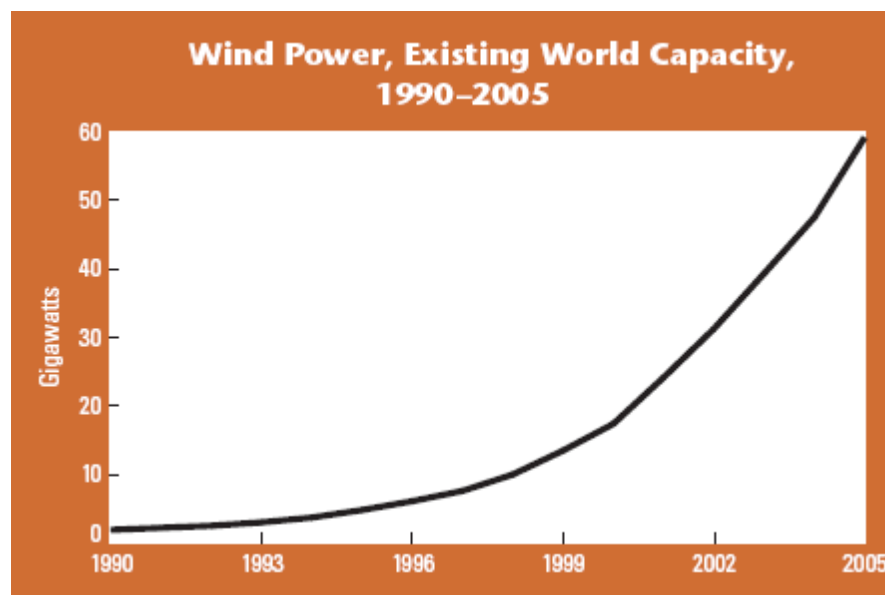


Figure 1-World Wind Power Capacity (Renewable Energy Policy Network, 2009)

Almost one hundred percent of the world's wind power is currently produced using wind turbines. While simple in design and implementation, turbines have many disadvantages. Firstly, the performance of a wind turbine is dependent upon the size and height of the turbine blades. In order to effectively use the higher, more constant wind flow at higher altitudes, large expenses are dedicated to constructing massive support structures in order to support the weight of the blades and generator. The blades themselves, sometimes reaching 90 meters in length, are difficult to transport. Transportation fees alone can now reach up to twenty percent of the total

equipment expense. In addition, wind turbines are inherently inefficient; to achieve an efficiency of forty percent is uncommon. Wind power is intermittent as well; performance in a wind turbine may increase or decrease dramatically over a short period of time with little or no warning. Due to these disadvantages, large wind farms need to be constructed in strategic locations in order to make their implementation cost effective. These wind farms take up a lot of airspace, are considered by many to be aesthetically displeasing, and create a high level of noise pollution during operation.

Recent studies have been investigating the feasibility of using large kites to harness wind power as an alternative to wind turbines. The most advantageous feature of using kites is undoubtedly the design's enormous performance potential at high altitude. Unlike turbines, kites support their own weight while in flight and do not require massive support towers to access higher altitudes. Thus, kites can be theoretically used to effectively harness wind power at heights where wind flow is much faster, cleaner, and consistent, where the limiting factor is simply the length of the kite tethers. The following equation shows that wind speed increases following a 1/7th power law, where y denotes altitude and V is velocity:

$$V = y^{1/7}$$

The following figure shows the effect of altitude on power as it increases proportionally to the cube of wind speed (Buckley, 2008).

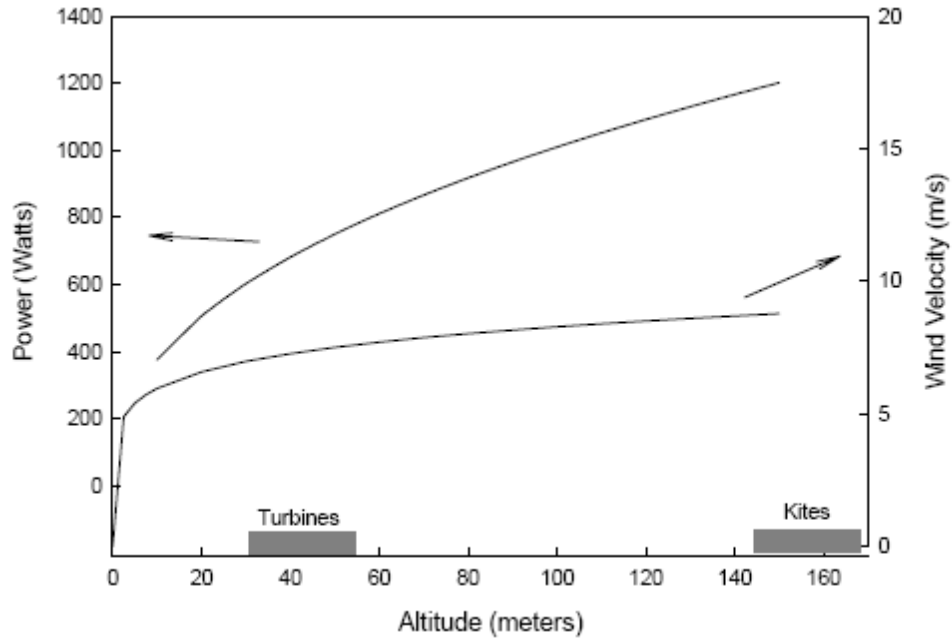


Figure 2- Power output and wind velocity for turbine and kite of 10 m² area (Buckley, 2008)

The potential for greater performance along with lower equipment costs may make the kite alternative a viable solution for communities in developing countries that do not have access to a power grid and cannot afford other options.

The goal of this project is to expand upon the work of two previous MQP groups in order to create a functional, one-kilowatt scale kite power system. While the previous groups have successfully built and proved the feasibility of the system, this project will focus on refining the design to optimize safety and efficiency, as well as install a series of instruments in order to evaluate and better understand the performance of the demonstrator.

5. Background

While energy has been extracted from the wind using turbines and windmills for centuries, the concept of using large kites to generate power has only been a topic of research in recent years. In the late 1970's, M. L. Loyd began to explore the potential for generating large-scale power using aerodynamically efficient kites. Loyd derived equations of motion for kites flying transversely to the wind at high speeds and was able to apply those equations to various airfoils. By comparing his results to newer technology, such as wind turbines, Loyd was able to predict feasible power production. Loyd was able to show numerically that a 2000 square meter kite had the potential to produce 45 megawatts flying at an altitude of 1200 meters (Loyd, 1980).

Dr. J.S. Goela is another individual who has spent many years focused on the research of kite power. While at the Institute of Technology Kanpur, Goela investigated the potential to translate kite motion to power generation. Goela's work was published in several journals and yearly reports during the 70's and 80's. Many of his ideas served as the foundation for this project and Dr. Goela has also served as a technical consultant on this project and interacted directly with the MQP project team. Goela was interested in proving, through experimentation, that kites could be used to translate wind energy to mechanical energy. He developed equations of kite motion and was able to use them to project potential power generation.

In the paper, *Wind Energy Conversion Through Kites*, Goela examined the dynamics of kite motion. He broke the cycle into two parts – kite ascent and descent. During the ascent phase, the kite is released, and during this stage, power is produced. During the descent, the kite returns to its original position and work is done on the system. Goela concluded that the power coefficient during ascent is at its maximum when there is a large lift to drag ratio. He also noted

that when the kite flies directly against the wind during the descent, the power coefficient is minimized (Goela, 1983).

In the same publication, Goela discussed the feasibility of using a kite system to power a pump. He broke the system down into three parts; “(i) a kite which intercepts wind at higher altitudes (ii) a nylon cord which transmits power from the kite to the base, and (iii) an energy conversion system located on the ground (Goela, 1983).” The design, as shown below, consisted of a balanced beam that was free to rotate about a hinge with spring loaded-assists. The kite was attached to the beam by two tethers and the displacement of those tethers could change the kite’s angle of attack. In the case of the pump, the conversion system was a bucket that could be filled with water. His work is worth noting because his conceptual design heavily influenced the final design for our kite power system.

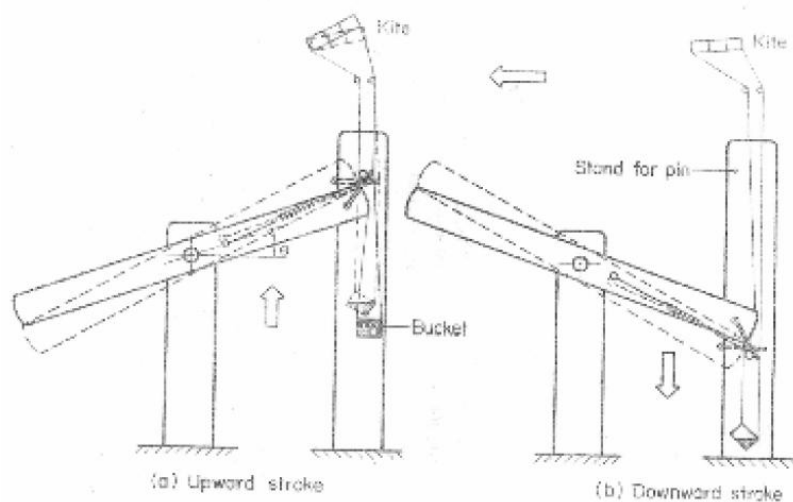


Figure 3 - Kite Pump System (Goela, 1983)

Italy has been the site of more recent work in the field of kite power, where researchers have focused on the Kite Wind Generator project. The Kite Wind Generator, or Kite Gen for short, is estimated to have the potential of generating as much energy as a nuclear power plant at a

thirtieth of the cost per megawatt. Kite Gen relies on a “carousel” of large, light-weight kites to generate power. The direction and angle of each kite is controlled by cables which result in rotation about the core. This activates large alternators and produces current (Martinelli, 2006). Recent testing was conducted at 800 meters above sea level, a height at which a Kite Gen power plant would possibly operate. An illustration of Kite Gen is shown in the figure below.

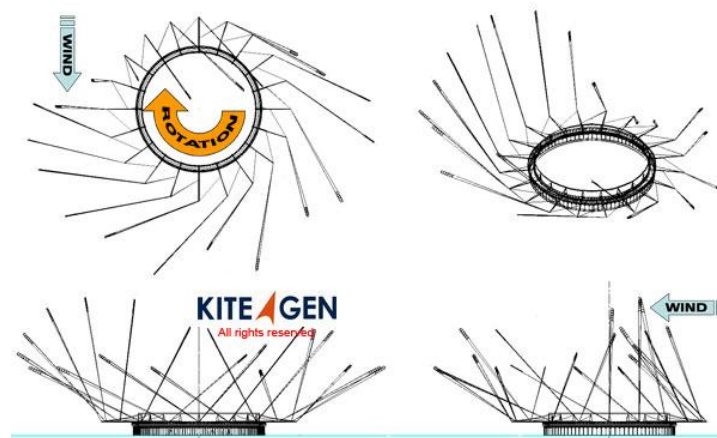


Figure 4 – Kite Gen Schematic (Kite Gen, 2008)

Kite power has been studied at Worcester Polytechnic Institute through MQP projects since the fall of 2006. The first project team (Blouin et al., 2007) focused on conceptual design analysis and looked at various kite power designs before deciding on a rocking arm design which was influenced by Dr. Goela’s work. The team was also responsible for testing numerous kites before concluding that a kiteboarding kite was best for application.

Their initial investigations laid the foundation for the subsequent project team whose work focused on building the kite power apparatus, as shown in Figure 5. They constructed a six-foot tall A-frame structure out of 4 x 4’s to serve as the core of the kite power system. A hollow metal rocking arm with detachable ends was mounted to an axle at the top of the A-frame. At the base of the A-frame, a gear train was assembled. A kiteboarding kite was attached to the end

of the rocking arm. Then, by attaching that end of arm to the power system, the motion of the kite could be translated into mechanical power. The mechanical energy can also be transferred into electrical energy through a generator and stored in battery banks. Finally, the focus of the project this year was 1) instrumenting the system to identify exact power output as well as system inefficiencies, 2) strengthening the structure, 3) lab testing, and 4) implementing safety precautions.

6. Project Objectives

The goals of this project are as follows:

- Design a data instrumentation system for a one kilowatt kite power system developed previously at WPI, accurately measuring:
 - Torque
 - Angular Velocity (RPM)
 - Rocking Arm Angle
 - Force of Kite Tether Tension
- Improve existing kite system from a previous 2007-2008 MQP Project
- Design & construct a 2nd power system that extracts power during the decent of the kite rocking arm on the kite power demonstrator
- Test structure and subcomponents over a range of expected conditions through lab and field testing
- Compare instrument data with theoretical results and conclusions

7. Design Process

7.1. Kite Power Demonstrator

7.1.1. System from 2007-2008 MQP



Figure 5 - Final Design and Equipment of 2007-2008 MQP Team (Buckley, 2008)

Upon completion of their project, the 2007-2008 MQP Team (Buckley, 2008) was able to successfully utilize kites to harness wind power. In doing so they were able to show that it is a feasible and desirable way to produce power. The team further developed the kite control system to allow for a more autonomous operation, in the hopes that future groups could further develop the controls to a point where the kite can fly on its own for extended periods of time. They were however unable to attach the control to the angle of attack apparatus and thus did not get to test the system in an autonomous configuration. Also, Professor Olinger added an operator chair within the system (also for autonomous control) in the following summer. The team also implemented a power train system on the structure that transferred kinetic energy generated by the wind into electrical energy by using the oscillating motion of the rocking arm to turn a generator. The developments moved the project closer to an apparatus which could be used to

harness power from the wind in developing regions of the world. In their final series of tests, the 2007-08 team succeeded in proving the ability of the system by harnessing wind power with a kite and using the natural mechanical energy to turn the power train and create electrical energy with a generator (Buckley, 2008).

7.1.2. Redesigned System



Figure 6 - Final Redesigned System

While much of the initial structure was made by the previous MQP teams from 2006-2008, our goal was to improve upon the structural integrity for additional field testing as well as add provisions for instrumentation for data collection and analysis. The steps taken to reach the final design for our project are explained in detail in the following sections. These steps include: designing and implementing several important safety features, structurally reinforcing and

refining the A-frame and the drive train set up and components, designing a secondary power system that allows for power to constantly be transferred to the drive train, fabricating aluminum parts for the oscillation control system, and installing and calibrating several instruments in order to evaluate the performance of the system through a data acquisition system.

7.2. Data Acquisition System

One of the main objectives of this year's MQP was to implement a data collection system to measure and record various parameters of kite power system. Not only did we want the ability to measure simple quantities such as the force felt on the lever arm by the kite tether, but we also wanted to determine more complex parameters such as how much power could be produced by the system overall. To do this, we turned to various types of instrumentation.

7.2.1. Key Measurements

Before purchasing expensive sensors, it was necessary to determine which variables needed to be evaluated in order to measure the power output and mechanical efficiency of the system. By measuring the power generated at the lever arm axle as well as the power generated at the drive shaft at any given time, we could determine the mechanical efficiency of the system. To calculate power this we used the kinematics equation of power for rotational systems,

$$P(t) = \tau(t)\omega(t)$$

where τ is torque and ω is angular velocity.

To determine the power generation of the larger axel, as shown the figure below, two measurements were necessary - the perpendicular force of the kite tether on the rocking arm and the angle of the lever arm. The angular velocity of the arm could be deduced from the change of angle of the arm over time.

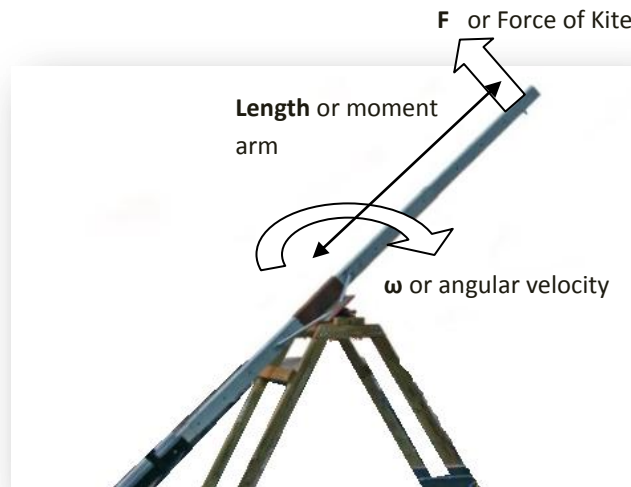


Figure 7 - Basic Measurements of Rocking Arm

To measure the power output at the gear train, two more measurements were necessary – the torque on the shaft connected to the generator as well as the rotation speed of the shaft. These two measurements could easily be obtained with a torque meter and a tachometer. With only four measurements many conclusions could be drawn about the system’s power generation capacity as well as its mechanical efficiency.

7.2.2. Instrumentation

Once it was clear what measurements were necessary to determine power output, instrumentation options were researched. Key parameters for selecting sensors included having analog output (necessary for our means of signal processing), size, measurement capabilities, portability, ability to withstand field conditions, required source voltage and cost. After researching various companies and products, we purchased four pieces of instrumentation as well as a data acquisition board to process the sensor signals. Below is a table of the sensors that were purchased for data collection:




Measurement	Instrument	Make	Model	Cost	Photo
Force (lbs)	Load Cell	Transducer Techniques	THB-1K	\$485	
Inclination (degrees)	Inclinometer	Rieker	N4	\$132	
Torque (N*m)	Torquemeter	Cooper Instruments	LXT-971-17.5NM	\$1395	
Shaft Speed (RPM)	Magnetic Pick-ups	Concept 2	N/A	Donated	

Table 1 - Instrumentation Purchased for Data Collection

7.2.2.1. Measuring Torque

One of the measurements required in order to fully assess the power of the system was torque. There were two options to consider when choosing what torque meter to purchase. The first option was buying a torque meter to measure the torque created by the rocking arm. The second option was to get one for the shaft of the flywheel. Using two calculations of torque, we approximated the torque at both the arm axle and on the flywheel shaft:

$$\tau_{arm} = r * F * \sin\theta \quad \text{where } r \text{ is radius, } F \text{ is force}$$

$$\tau_{drive} = I_{fw} * \alpha \quad \text{where } I \text{ is moment of inertia of flywheel, } \alpha \text{ is angular acceleration}$$

The torque on the arm is a moment equation. Essentially, the kite tether is attached to the end of the arm by an I-bolt. In the table below, the estimated torque is calculated:

Length of Lever Arm (m)	1.83
Estimated force on Arm due to Kite (N)	889.644323
Estimated Torque (N*m)	1628.049111

Table 2 - Table of Arm Torque

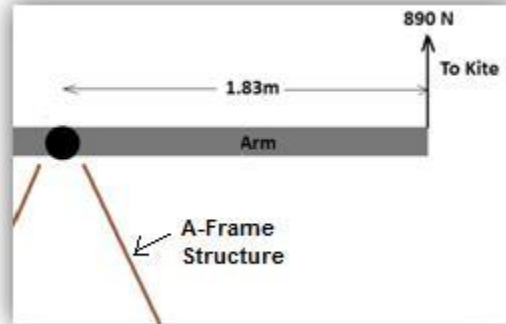


Figure 8 - Illustration of Force on Kite

The torque on the drive shaft system is more complicated, which involves the moment of inertia of the flywheel as well as the angular acceleration of the shaft. This number can also vary between the two different size flywheels that can be used. Using mechanics equations, these values were estimated. Below is table of the resulting estimated torque calculations:

	Large Flywheel	Small Flywheel
Mass of Flywheel (kg)	20.4	11.3
Diameter of Flywheel (cm)	44	26.9
Moment of Inertia (kg*m ²)	0.483	0.103
Angular Acceleration of Flywheel (rad/s ²)	10.22	10.22
Estimated Torque (N*m)	4.93626	1.05266

Table 3 - Table of Drive System Torque, depending on size of flywheel used (Buckley, 2008)

From these calculations, the team found it more reasonable to measure the torque on the shaft of the drive train.

7.2.2.1.1. Initial Setup

To measure torque, the team purchased a LXT- 971 shaft-to-shaft torque sensor. It is rated up to 17.5 Newton-meters, which, according to the estimated calculations found earlier, was more

than enough of a safety factor to handle the torque of the shafts. However, due to many factors that could contribute to added resistance such as pulleys and bearing mounts, the team wanted to be as safe as possible as to not compromise the pricey sensor.

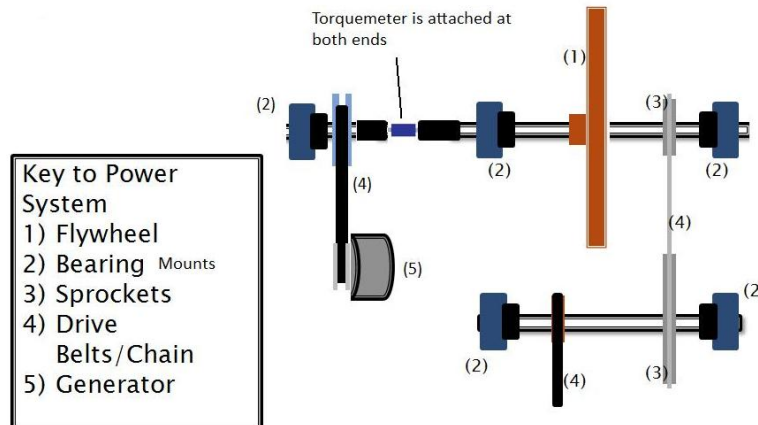


Figure 9 - Diagram of power train setup with torque meter

The design intent for the torque meter was to attach it directly to the flywheel shaft, between the generator and the flywheel. In order to attached these pieces, two aluminum couplings were turned on a manual lathe with an inner diameter of 1 inch for the steel shaft and 0.355 inches for the torque meter shafts. Each piece was also fitted with set screws to hold it in place. The picture below is a Solidworks assembly of the intended setup:

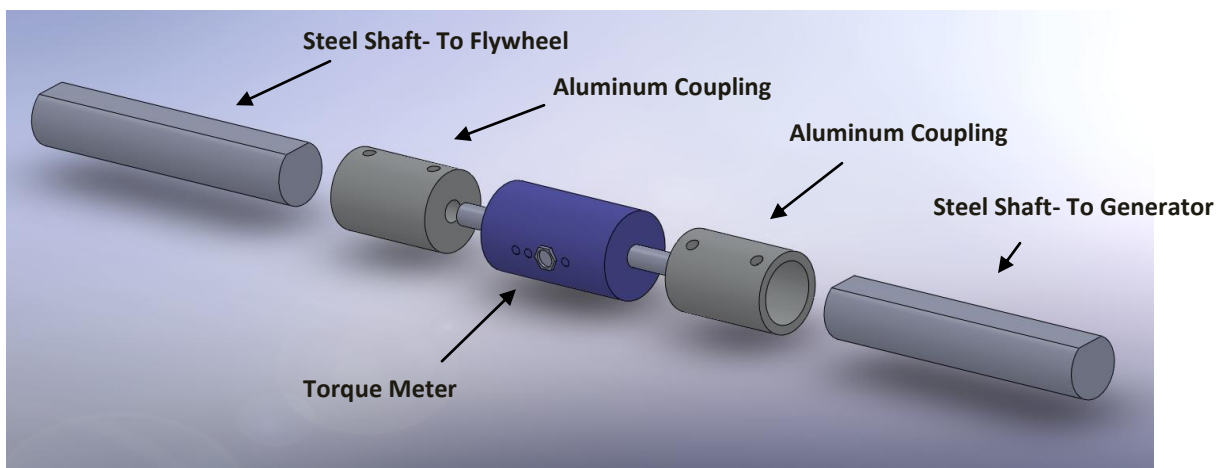


Figure 10 - Solidworks Assembly of general layout of Torque meter setup

These shafts were mounted through two bearing mounts. Along with the couplings, a fixture also had to be created that would hold the torque meter in place as the shafts moved. A simple design was created from two pieces of plastic where the torque meter's geometry could create a slide fit with placement screws. This was to maintain the design intent of making the "holder" easy to assemble and disassemble. Below is a Solidworks model of the holder.

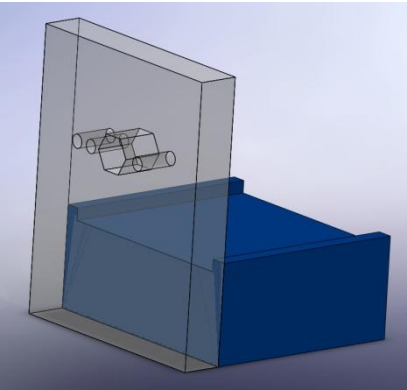


Figure 11 - Solidworks model of torque meter fixture

The initial design with all pieces can be seen below. This configuration has a pulley attached on one end that is connected by a belt to the generator.

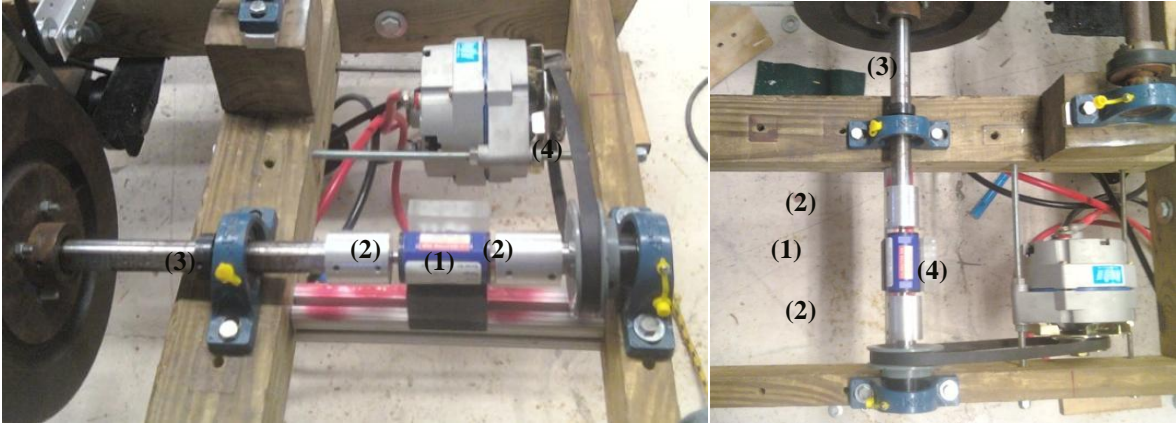


Figure 12 - Initial setup of (1) Torque meter (2) Couplings (3) Flywheel and (4) Generator

7.2.2.1.2. Friction Reduction/Final Design

Through a few preliminary mechanical tests with the initial setup of the torque meter and generator, there was a substantial problem with the first setup. The friction of the belt from the generator to the pulley at the end of the torque meter was more than expected. The belt/pulley would cause a frictional load in the lateral direction of the shaft, increasing the inertial force, causing the shaft to resist motion and quickly stop rotation. There were also signs of belt slippage and dramatic speed reduction. This was a large issue in terms of power production.

The team decided that rather than transferring the energy through a pulley, the generator could be placed directly on the flywheel shaft. This would eliminate any excess friction on the system and provide a better means to attach any sort of sensor on the shaft, between the flywheel and the generator. A diagram of the setup can be seen below:

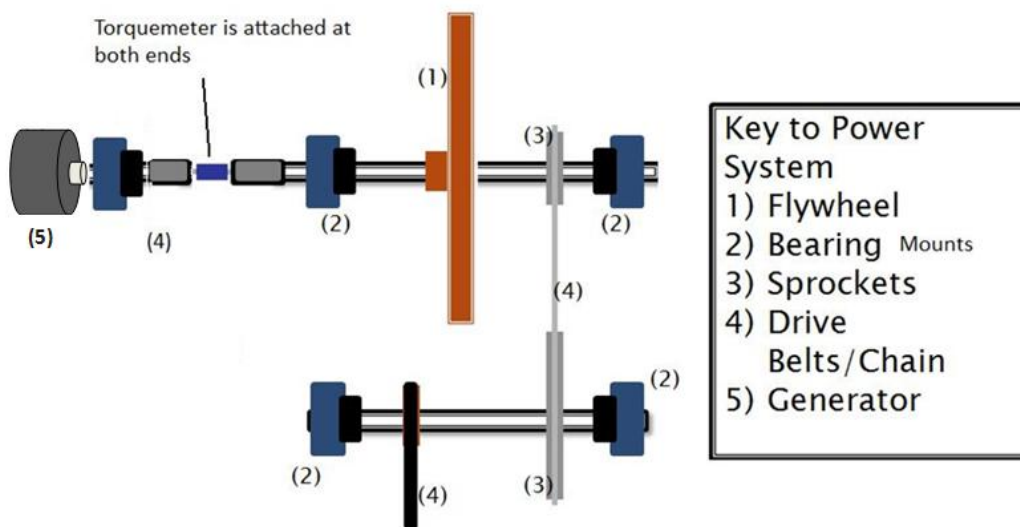


Figure 13 - Diagram of Final Setup (direct coupling to shaft)

A new fixture had to be built as the generator was to be moved outside the A-frame. It was created to be assembled and disassembled with ease. Below are pictures of the final design setup:

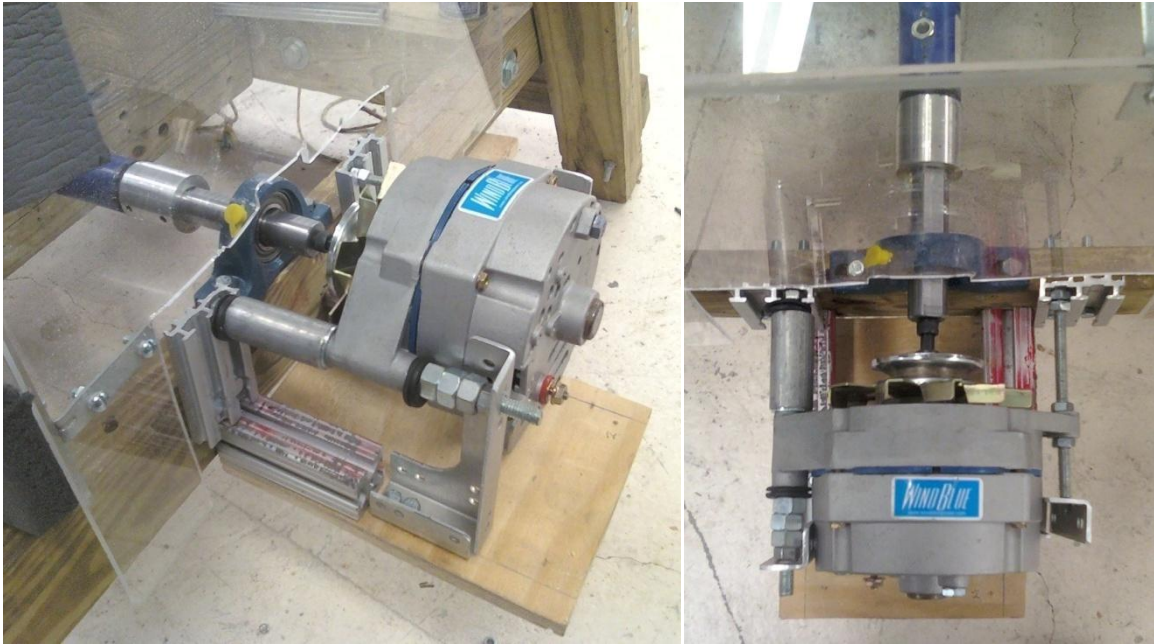


Figure 14 - Generator with added fixture for shaft-to-shaft setup

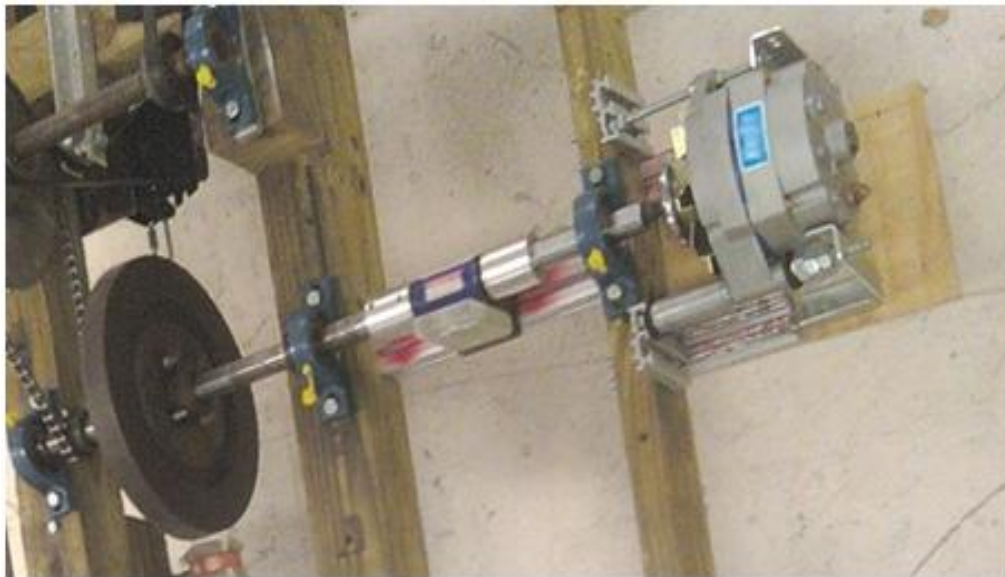


Figure 15 - Final Setup of Torque meter and Generator

7.2.2.2. *Measuring Kite Force*

In order to measure the force of the kite on the arm, we purchased a Transducer Technique THB thru-hole load cell. This model was a donut shaped cell with a capacity to

measure compression up to 1000 lbs. The max load of the load cell was chosen based on the calculations of the 2007-2008 MQP team who found the tether force to be in excess of 200lbs (Buckley, 2008). The load cell outputs a voltage when the cell is compressed. The design intent of using a compression load cell was based upon the force that the kite tether puts on the I-bolt at the end of the arm. The I-Bolt would be pulled upward and would put compressive stress on the nut and washer on the other end. To accurately read the force, the load cell could be placed between the nut and the I-Bolt to accurately measure force (see following figure). Also, in order to avoid bending of the square frame of the arm, a system of spacers were used to fill the gap.

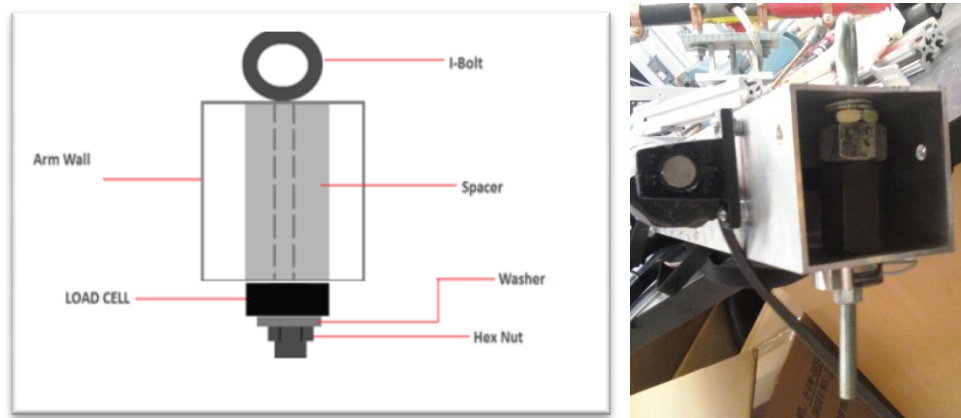


Figure 16 - Diagram and photo of Load Cell configuration

7.2.2.3. *Measuring Rotational Speed of the Flywheel Shaft*

In order to measure the rotational speed of the flywheel shaft (or angular velocity), the team needed a tachometer. In our search, we were unable to find a suitable sensor that would give minimal interference and a continuous voltage output. Through talks with Concept 2, a well-known rowing machine manufacturer, they gave insight for our system based on measuring the internal rotations per minute (RPM) of their rowing machine flywheel. They were gracious enough to donate the magnetic ring and pick-up from their system. The ring has twelve magnetic

poles. It would be as if six magnets were in a ring. The magnetic pickup produces a pulse every time a pole passes by. The magnetic ring, as can be seen in the figures below, is attached to the flywheel shaft by a plastic mount. The mount was created by placing a 4in diameter piece of plastic in a lathe and turning it to the desired shape, while also cutting a 1 inch diameter hole in which to place the flywheel shaft. The magnetic ring was secured by Velcro and the plastic mount was secured to the shaft by a set screw. The pick-up was secured to the frame by a simple structure that was designed to be adjustable and simple to remove.

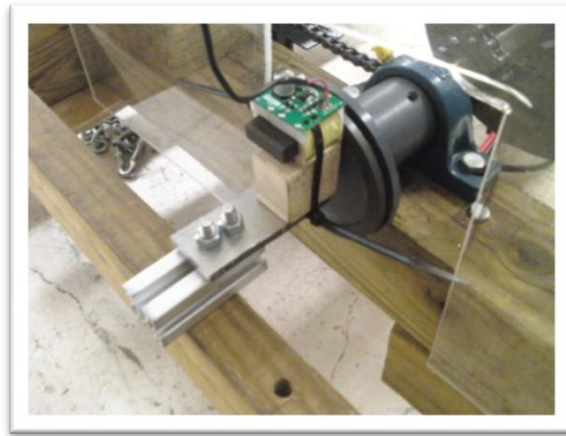


Figure 17 - Tachometer setup on system

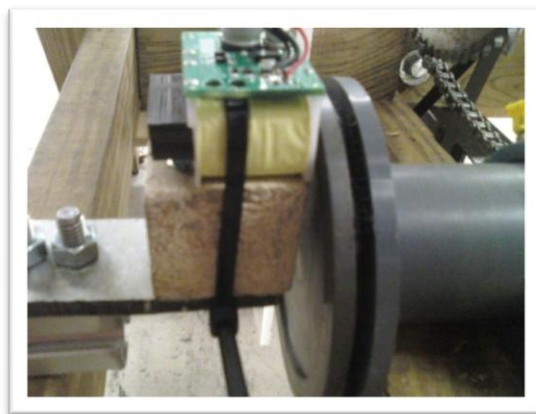


Figure 18 - Pickup and magnetic disc in close proximity

7.2.2.4. Measuring Inclination

For the angle of the lever arm, we purchased a Rieker N Series inclinometer. In its series, it was meant to be durable, with an error factor of $\pm 0.01^\circ$ with a total range of $\pm 70^\circ$ of inclination. The inclinometer was a liquid capacitive gravity-based sensor with an analog output. The natural inclination of the arm is like a see-saw, where the max angle would never breach $\pm 35^\circ$; this would be more than enough rotation clearance to collect accurate angle readings.

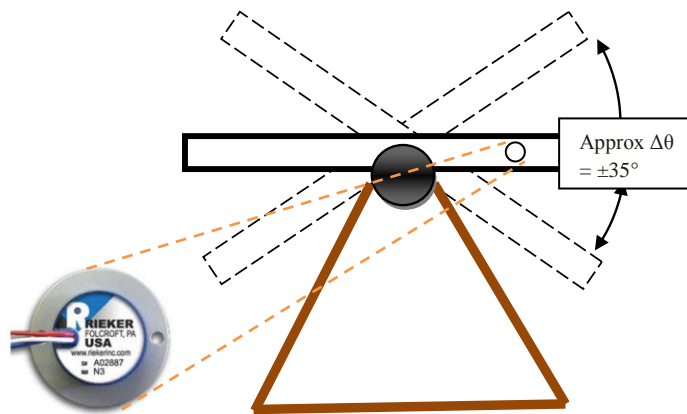


Figure 19 - Rieker Inclinometer and Illustration of Maximum Arm Angle

As seen in the picture above, the inclinometer would have to be placed directly on the arm. However, it had to be attached in such a way that it could be removed with ease and protected from weather conditions. Our team created a Solidworks assembly of the inclinometer fixture that could be attached to the arm:

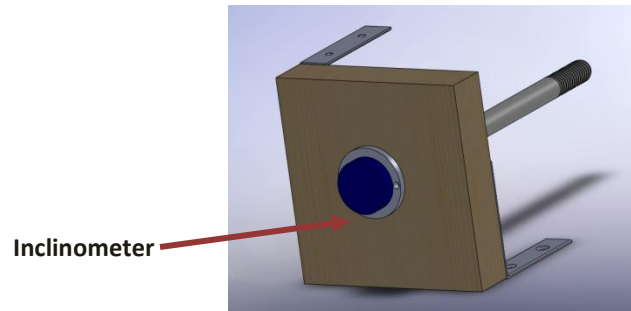


Figure 20 - Solidworks Model of Inclinometer Fixture

As seen in the picture, the inclinometer would be attached to a piece of wood that would be bolted to the arm and tightened by a nut on the other side. However, it still needed a covering. Therefore, a piece of Tupperware was fitted on top, which could be screwed on and off for easy access. The wires are then fed out a hole in the side of the plastic Tupperware to the DAQ board.



Figure 21 - Final Setup of Inclinometer on the Rocking Arm

7.2.3. Calibration

Each instrument was tested and calibrated in the lab before being mounted onto the kite system. To process the sensor outputs, we purchased a low-cost, USB based, portable data acquisition (DAQ) board from National Instruments and configured it on a laptop that could be used for lab and field-testing. LabView, a program used for measurement and automation, was

installed on the laptop to read the DAQ board channels. All four pieces of instrumentation provided analog outputs with milli-volt or voltage readings and could be processed using the DAQ board and LabView.

The inclinometer was tested in Higgin's Experimentation Lab before being mounted to the lever arm. The inclinometer required a source voltage of five volts which we ended up drawing from the DAQ board itself. The sensor came with a calibration sheet that was used to translate the voltage reading to an angle measurement. Once calibrated, the inclinometer was fixed onto the lever arm inside of a Tupperware container for weather proofing purposes. The sensor was zeroed by subtracting the offset voltage that was read when the beam was level. Wires were run in plastic tubing from the sensor to the location where the DAQ board would be mounted to the A-frame.

The load cell was first tested in the lab by using a large clamp to apply a compressive force. The load cell required a nine-volt source, which was provided by a battery. While we were successful in obtaining millivolt readings, we did not know how to interpret them because the load cell did not come with a calibration sheet. To calibrate the load cell, we worked with the Civil Engineering department and used their Instron compression machine to determine the calibration factor. As the Instron compressed the load cell, mV readings corresponding to various known load were recorded. A graph of that data is below. Using that chart, a calibration factor of 50 lbs to one millivolt was determined using a line of best fit. The correlation of the data was 0.9994. Later, the calibration factor was verified by the manufacturer.

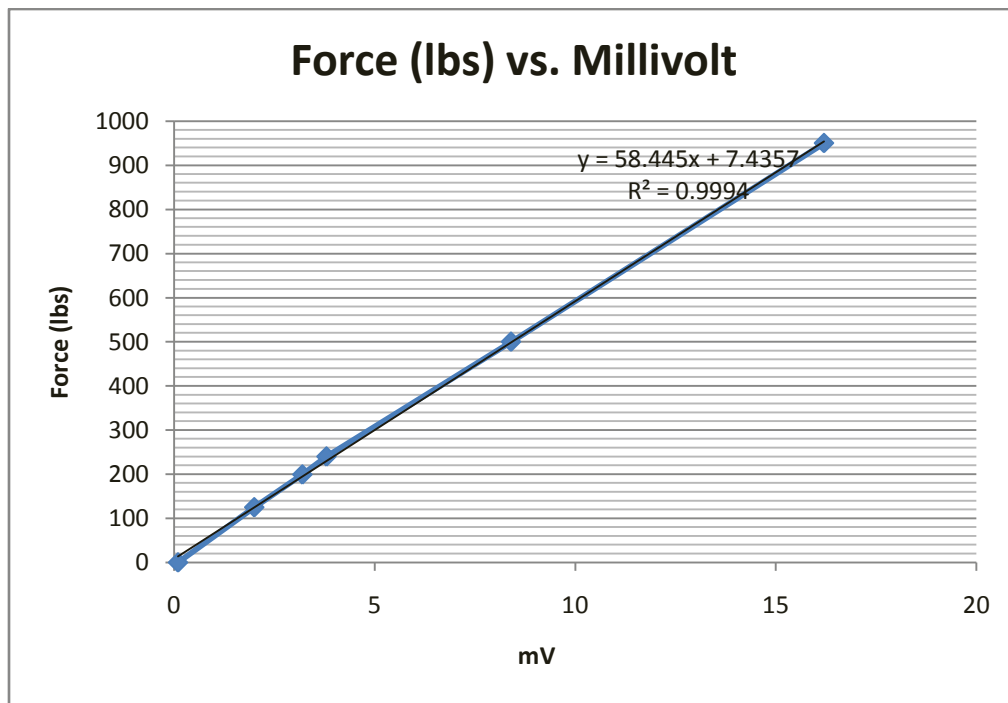


Figure 22 - Graph of Force per millivolt of the Load cell

Once the load cell was calibrated, it was connected to the DAQ board to ensure that it would read in LabView. Once it was set up, we noticed that there was a considerable amount of noise

that made the measurements almost meaningless. We determined that the resolution of the portable 12 bit DAQ board was not great enough to read both millivolt and voltage signals. We worked with Transducer Techniques Technicians who suggested we purchase an amplifier to condition the signal to output +/- 8 V opposed to +/- 20 mV. We purchased a model TMO-1 load cell signal conditioner which is shown in the figure below. An AC power adapter was also purchased for the amplifier to take care of the 12 Volt source requirement. The adapter was purchased with the intent of plugging it into the electrical board that was built by the 2007-2008 MQP team when out in the field (Buckley, 2008). Once the amplifier was correctly wired, it was fixed to the top of the DAQ board using Velcro to keep it in place.

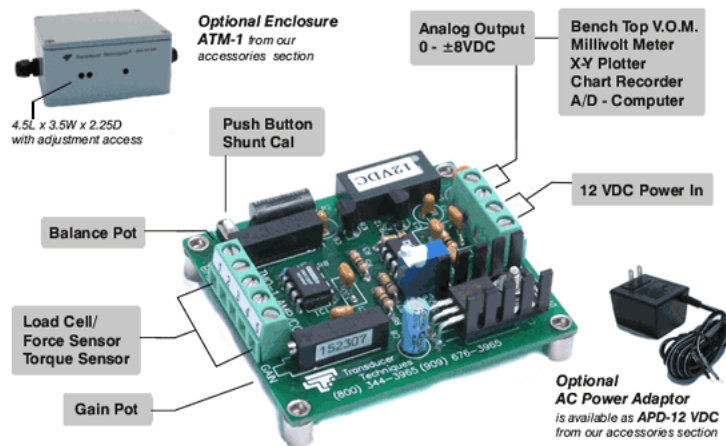


Figure 23 - TMO-1 Amplifier for Load Cell Conditioning

Because we were using set of magnetic pickups to measure the speed of rotation of the drive shaft, we had to calibrate the sensor by hand. First, we mounted the circular magnet to the drive shaft using a PVC coupling. Then we attached the pick-ups to a power drill with a maximum speed of 1400 RPM. Using LabView, we recorded the voltages corresponding to 0 and 1400 RPM. By assuming a linear voltage output, we determined the zero offset as well as the calibration factor for the magnetic picks ups.

Once the torque meter was mounted to the kite power system, it was fairly simple to calibrate. The sensor came with a calibration sheet which provided a calibration factor that could be used to translate the raw voltage signal to a N*m measurement. The sensor was zeroed by subtracting the initial voltage offset and the calibration factor was added to the LabVIEW sequence to obtain the final torque measurement.

Once all four instruments were calibrated and fixed onto the kite power system, the sensors were rewired to make it easier to connect them to the DAQ board. The DAQ board was mounted into a small metal box on the inside of the A-frame using Velcro. All the sensors were rewired with servo connectors so that each instrument could be easily connected or disconnected. This setup not only allowed the data collection system to be set up quickly, but also eliminated the possibility of incorrect wiring. A photograph of the DAQ board with the connectors is shown below in the following figure.



Figure 24 - Photo of Wiring setup of DAQ and instruments

7.3. LabVIEW

To interpret the sensor output signals we developed a VI in LabVIEW. We worked closely with Professor John Sullivan to create our program so that all four measurements could be processed simultaneously. We were able to arrange the VI such that all four measurements could be displayed on graphs in real-time. Another important feature of the program was that it was able to write the data to a spreadsheet with the click of a button. Below is a screenshot of the VI front panel.

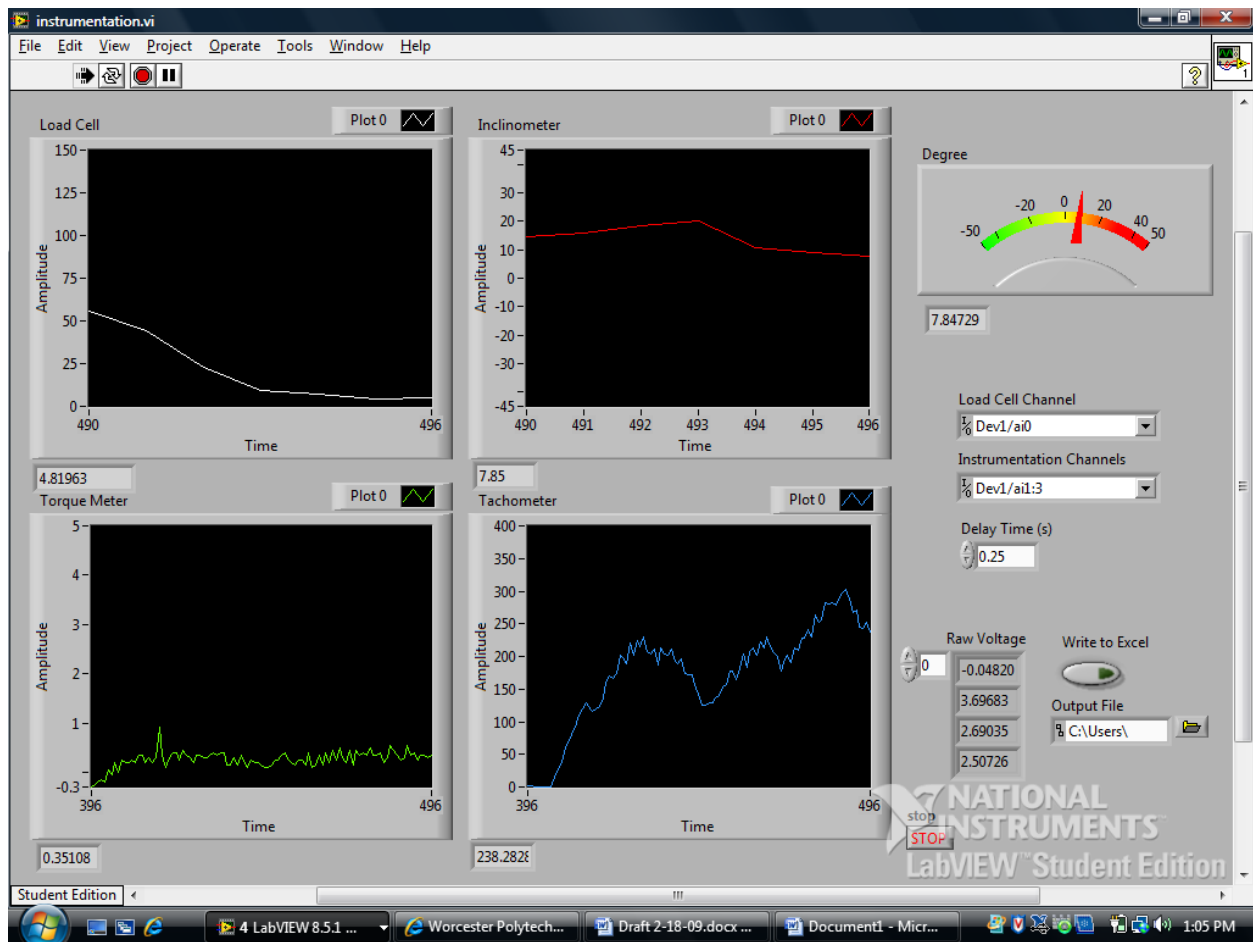


Figure 25 - LabVIEW Front Panel

The VI was configured to read analog voltage outputs within a 'while' loop. The four signals were separated by assigning each to its own channel. Raw voltage readings for each

instrument were arranged to be displayed on the front panel. The measurements were then numerically manipulated to translate voltage readings to force in Newton's, degrees, torque in Newton-meters, and RPM. Graphs corresponding to each measurement were added to the front panel to display readings in real time. All measurements were then fed to a Boolean loop containing a write to spreadsheet command. A spreadsheet format was set up to track time, force, inclination, torque and rpm. A 'write to excel' button was added to the front panel for easy recording during lab or field testing. A screenshot of the block diagram is shown below.

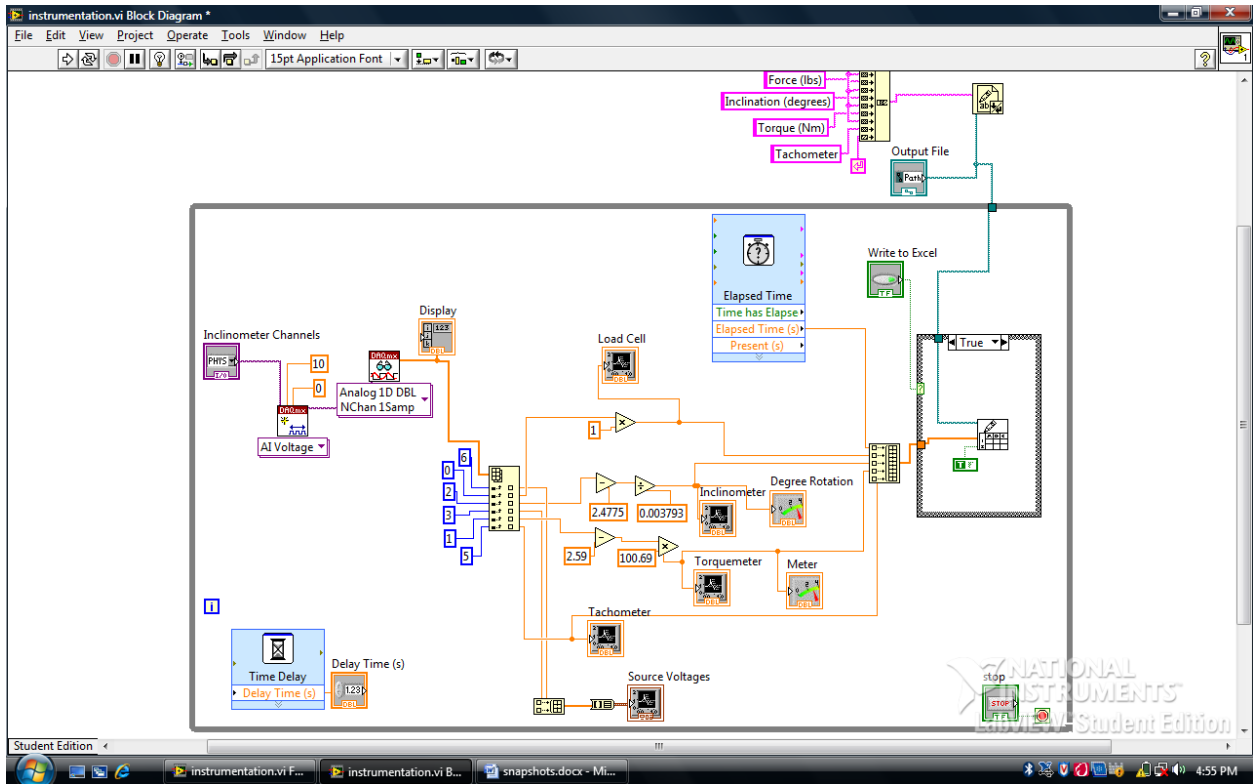


Figure 26 - LabVIEW Block Diagram

7.4. Structural Improvements

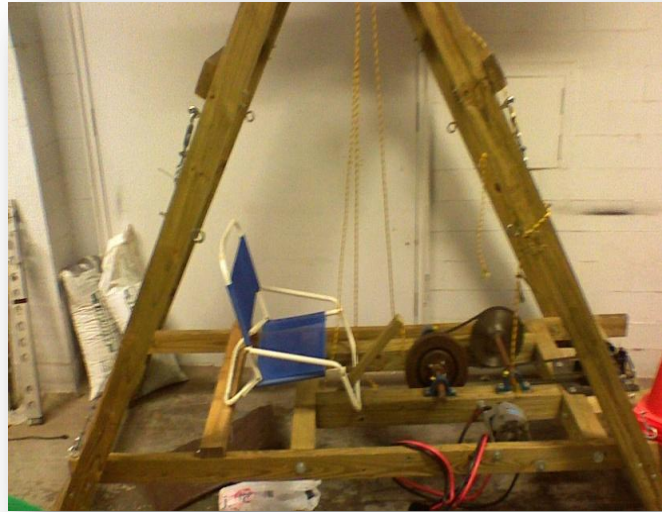


Figure 27 - Original A-frame Structure

One of the primary goals of the project was to improve the structural and safety features of the 2007-2008 MQP (Buckley, 2008). This initial design process came under three categories of improvement: structural integrity in the field, power conversion of the drive system, and safety of the operator(s) and team. Towards the end of the project, the team also had to implement further design changes to compliment the mechanics of the instrumentation. Overall, by improving the system, the team could optimize its longevity in sustained testing for future innovation.

7.4.1. Oscillation Control

The translational motion of the kite is crucial in harnessing its energy. The kite power MQP has seen several designs dedicated for the optimal control of the kite as it pertains to the power stroke of the rocker arm on the project's A-frame. While all of the designs have used the rocking motion of the rocker arm to power and de-power the kite by means of a gravity actuated

sliding mount for the control bar, only the current design provides means for controlling the kite throughout its natural oscillations on the lateral axis. Ideally, the design would include an autonomous control system so that the prototype could be left unattended during long periods of use, but considering the project's limited monetary budget, implementing the complex processor and servos required for such a complex system would not be realistic. The current design, devised by the 2007-2008 MQP and modified during the summer of 2008 by Professor Olinger, uses a sliding mount for the kite's control bar attached to a pair of rails that are mounted in parallel with the end of the rocker arm (Buckley, 2008). This prototype design can be seen in the figure below:

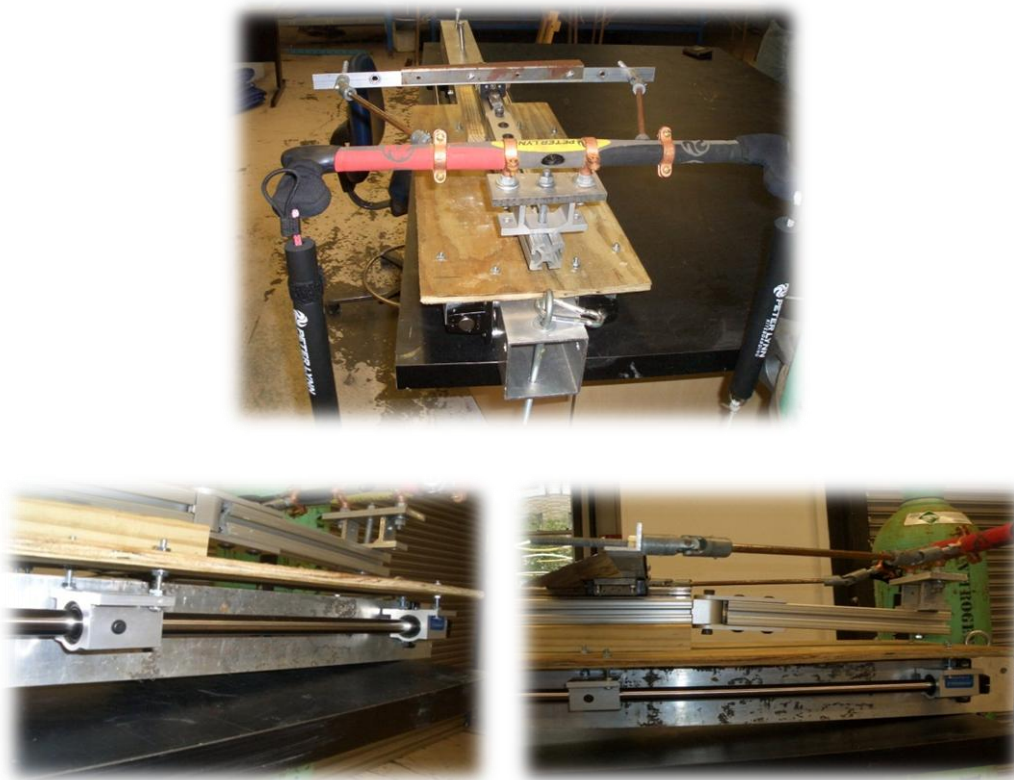


Figure 28 - Initial prototype of sliding mount for control

While gravity forces the mount to automatically power and de-power the kite as the arm rocks through its power stroke, a “pilot” is required to sit in a seat within the A-frame and fly the

kite through its natural lateral oscillation with a handle attached to the ends of the control bar via cables. The pilot can use the handle to steer the kite in order to keep a manageable, tight figure-eight pattern, combat erratic behavior resulting from unexpected wind gusts, as well as pull back on the mount in order to de-power the kite at will. The preliminary design featured a rough cut wooden mount and rudimentary fasteners that the team replaced with machined aluminum parts. The refurbished mount weighs fifty-two pounds and features a slot in the base plate designed to accommodate a spring that would fasten the sliding mount to the end of the rocker arm in order to, if necessary in the future, delay the mount from naturally sliding backwards and prematurely de-powering the kite as the rocking arm moves through its power stroke.

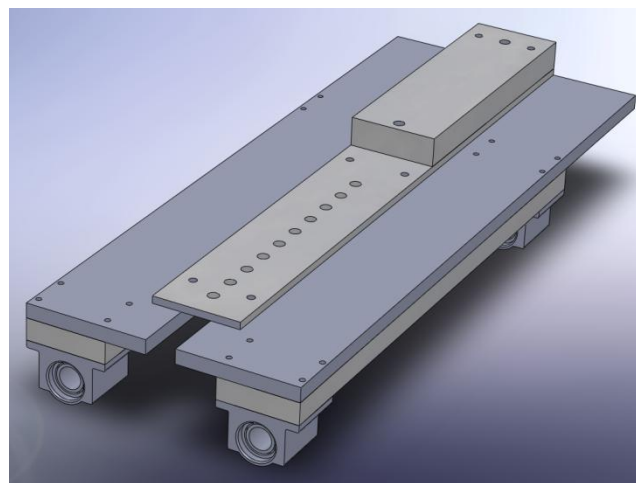


Figure 29 - Solidworks Model of Sliding Mount

The design features of the oscillation control piece focus on structural integrity as well as providing a counter weight to the rocking system. The aluminum oscillation piece (seen below on the arm) could handle the rigorous forces of the kite's motion. The over engineered aluminum base plate and spacing pieces provide a significant counter weight for the rocking arm and provide the energy needed for the secondary power system to turn the flywheel and generator during the arm's down stroke. The added weight of the mount puts a lot of stress on the slide

rails when it slams into its power and de-power positions during the rocker arms stroke. In order to alleviate the violence of the collisions and increase part life, the team added simple but effective foam dampeners to the rails.

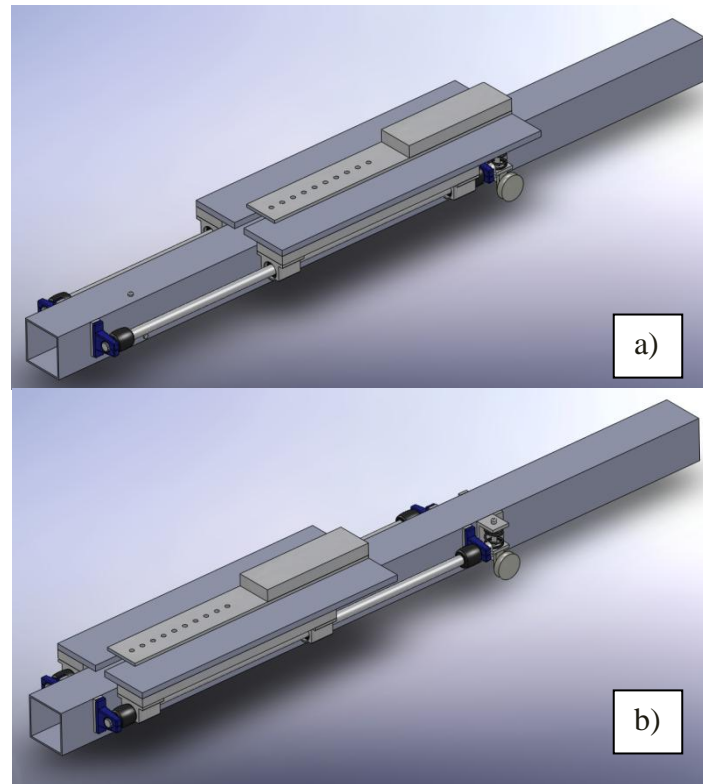


Figure 30 – Solidworks Model of Sliding Mount in a) Power Position & b) De-power Position

7.4.2. Moving the Power Train

With the addition of the operator chair, the gearing had to be moved to accommodate accordingly. As seen in the figure below, there was not enough room for the operator to sit comfortably and not be affected by the rotation of the flywheel. In order to accomplish this, the team raised the front gears on two wooden blocks and brought the flywheel and its bearing forward. Also, a new smaller drive belt was purchased and placed on the system. This gave the

driver an extra 5 inches of clearance from the power train. Also, this gearing placement allowed for the larger flywheel (20.4 kg) to be easily placed without much hindrance on the operator.

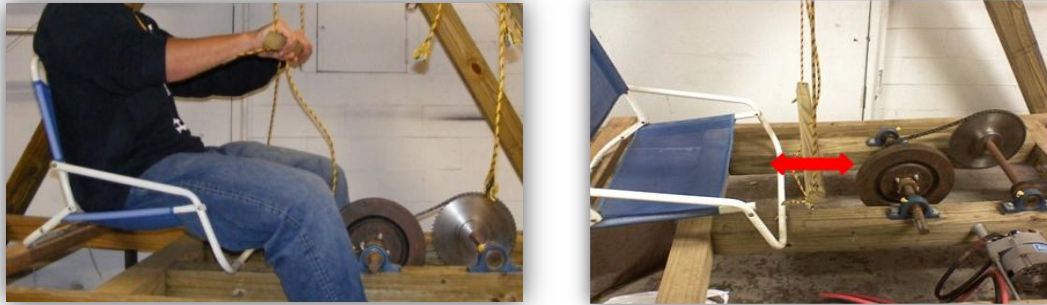


Figure 31 – Initial Proximity of Gearing to the Operator

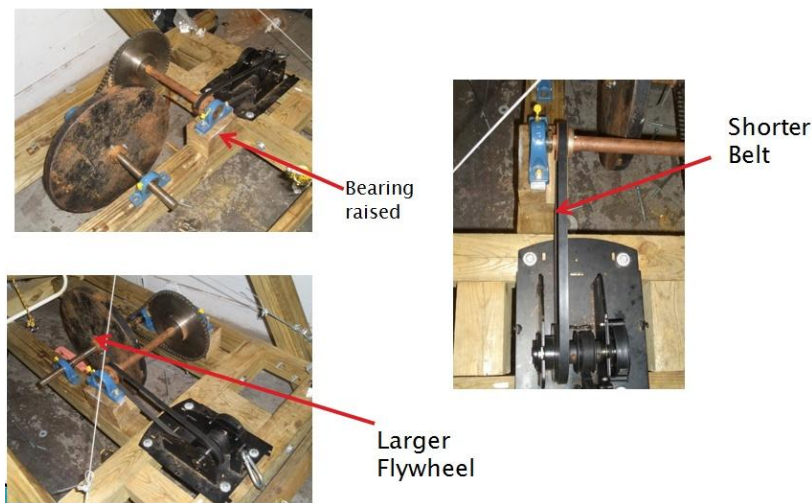


Figure 32 - Gearing Placement

7.4.3. Improving A-frame

The structure of the system was assessed by a simple physical check of the system, looking for weaknesses in the frame. From a physical standpoint there were apparent cracks in the structure along with a lack of stiffness in some areas. During our lab tests, the shafts would rotate and cause a substantial amount of vibration throughout the system. There needed to be more structural integrity to insure that the frame could withstand long cycles of testing.

Many large cracks were found coming from the many bolts and screws going through the 4x4 beam. From previous experiments, wear was apparent from the lateral force applied to the structure from the oscillation movement of the kite and arm.



Figure 33 - Wear on A-frame

A couple ideas were proposed to address this issue. The first idea was to take a piece of sheet metal cut in a trapezoidal shape and bolting or screwing it in multiple places on each side. It would secure both legs of the A-Frame to each other and the top section. Also a long rectangular section of sheet metal could be run laterally across the top of the frame to secure the two sides of the structure together. However, having a single piece would be hard to place with the amount of screws and bolts already present. It would also be a safety concern to the operator to have a large piece of sharp metal just above the entrance to the operator's chair.

The better possibility was to take heavier, thicker metal beams and building a cross beam and securing the metal to each other where they crossed. This would form an "X" on each side of the structure, with a bolt through the center of the "X" to secure the beams together and increase rigidity. It also would only require four bolts, or screws, on each side of the structure, which would be more ideal structurally and from a safety standpoint. A 12 foot piece of 2 ¼ inch X 5/8 inch steel was found and cut to length. Four 2 foot sections were cut along with four 3 inch section from the 12 foot piece. 3/8 inch holes were then drilled in each section of steel. The short

pieces were placed under one of the longer sections on each side in order to lift it away from the structure, so it could pass by the other long section, thus causing them to be flush against each other where they crossed in the center.



Figure 34 - A-frame with added cross reinforcement

The top points of the “X”s were to be secured to the structure with ½ inch screws, to the 3/8 inch holes were widened out to ½ inch holes. Also a 3/8 inch hole was drilled through the center of the long sections, then a short, 2 inch long 3/8 inch bolt was put through the hole to form the “X”s. After the “X”s was formed they were attached to the structure using 3/8 inch bolts on the lower points and ½ inch screws on the upper points. When this was done to both sides of the structure it was found to have greatly increased the strength and rigidity of the structure.

7.5. Power Conversion

One of the main goals of this project is to optimize power production from the system. The biggest area of improvement is to find ways to harness as much of this energy as possible to make kite power more efficient.

7.5.1. Second Power System

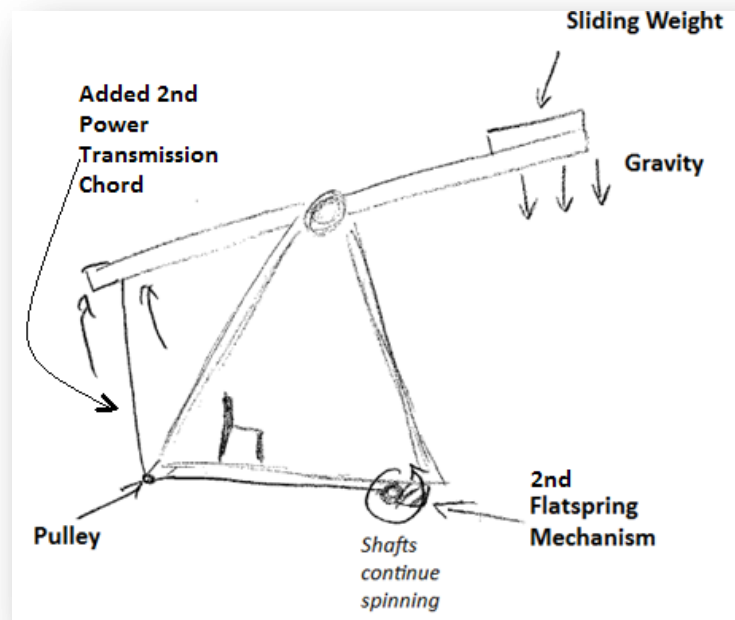


Figure 35 - Sketch of Second Power System

In order to further refine the demonstrator's power system, the team has implemented a secondary power system that applies torque to the flywheel whenever the rocker arm is moving. Unlike the original design which only applies power during the upward power stroke, the new system implements a second nylon cord attached to the opposite end of the rocker arm and uses the energy of the descent of the oscillation piece at the end of the rocker arm to turn the flywheel as the kite stalls and the arm lowers to the bottom of its stroke. The secondary power system uses a second identical flat spring rowing assembly that is directly attached by belt to the same axle.



Figure 36 - Flatspring Assembly

The system has shown satisfactory performance by both transferring constant and consistent power to the flywheel throughout the rocker arm's entire range of motion as well as slowing the arm's descent in order to relieve impact fatigue from otherwise violent downward movement of the oscillation piece. This secondary benefit should substantially increase part life; when the rocking arm's down stroke is not damped by the second nylon cord, the newly refurbished, fifty-two pound oscillation piece exhibits rapid movement when it slides back into its power position. The impact with the end of the slide rails puts a great deal of unwanted shear stress on the rail mounts.

Unfortunately, the secondary power system proved to have its share of problems before the desired level of performance was achieved. Firstly, the added friction created by the second belt and its tightening system has shown a substantial decrease in system efficiency. While the system retains a constant spinning of the flywheel whenever the rocker arm is in motion, the added friction keeps it from reaching and retaining the high angular velocities it was capable of without the added tether. Also, the secondary system uses the same gearing ratio as the primary system, and thus requires the same force to turn the flywheel. This force is substantial and if the forty-five pound flywheel is not already spinning, the mass of the oscillation piece is not enough to force the arm through its down stroke. To counter this problem, the team was forced to make several modifications the system in order to effectively implement the secondary power system.

Firstly, the team reduced the torque required to turn the flywheel by replacing the forty-five pound flywheel with a smaller twenty-five pound weight. The nylon cords that connect the rocker arm to the power system were then moved closer to the arm's fulcrum, thus increasing the system's mechanical leverage and reducing the force required to turn the flywheel. Lastly, satisfactory performance was achieved when the team alleviated the excessive frictional losses in the system by refining the alignment of the axels as well as repositioning the generator directly in line with the shaft that spins the flywheel. The final generator configuration negates the friction created by the lateral tension on the fly wheel shaft by removing the generator belt and allows the rocker arm to consistently perform a quick but controlled decent into its next power stroke.

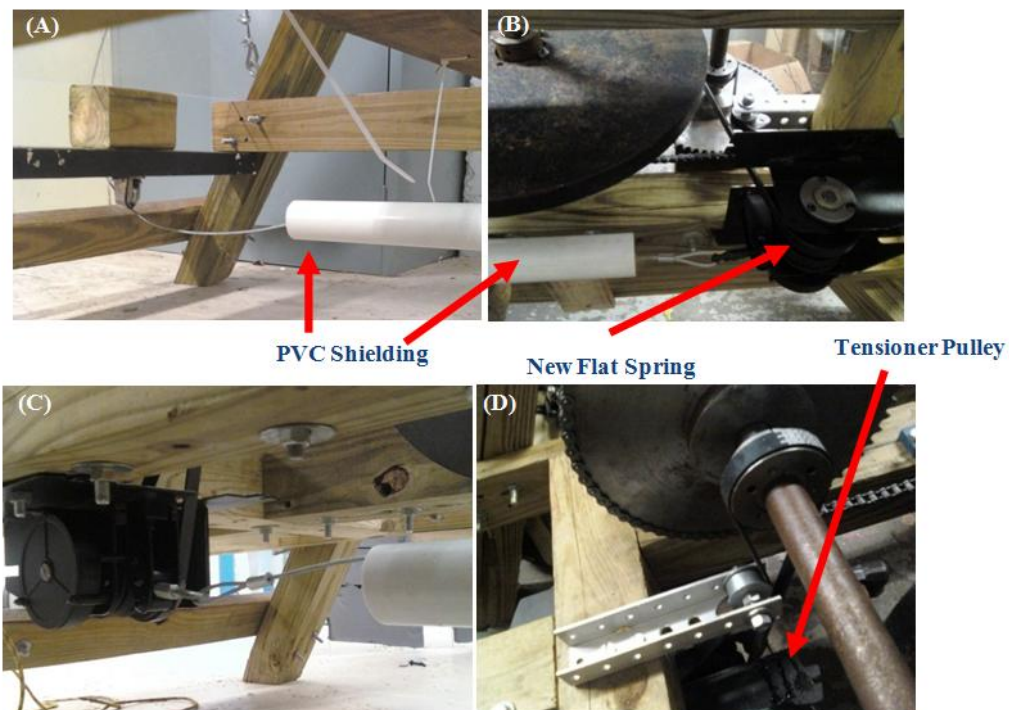


Figure 37 - Photos of Second Power System

The setup of the second power system consists of a flat-spring system taken from a rowing machine that was bolted to the under section of the A-frame structure. A belt from the flat-spring mechanism is attached to a follower pulley on the chain shaft which was in tension (D). Steel cable is used as the nylon cord which, when pulled, creates shaft motion. This cable is fed through a safe system of PVC piping towards the other end of the arm (A,B) where it is followed through two pulleys to be attached at the other end of the arm (A) .

7.6. Safety Improvements

With the addition of the operator seat component as seen in the figure 30, and the expectation of more rigorous field testing, safety became one of the most important components of the structural improvements process. A few measures were put in place to protect the project team from accidental injury while the system was static or dynamically operating.

7.6.1. Protective Guards

The project team designed a system of guards to further protect the operator. The purpose of the guards was two-fold. It would provide the operator safety from the large flywheel and gearing, as well as protect the entire gearing system from any foreign objects hindering the system. An acrylic enclosure was designed for the gearing that would provide a substantially protective covering of the gearing that would be “see-through” as well as added padding to the operator’s comfort. The enclosure consists of 4 pieces of $\frac{1}{4}$ inch clear acrylic plastic as well as HVAC duct padding. Due to the rigidity of the gearing, the team felt that protection from any of the gearing failing during operation or coming off its mounts was unlikely, and this type of plastic would be sufficient merely in a protective stance. The actual enclosure was modified in order to fit into the system, adding more cuts to wedge the box between the bottom wood planks as well as extra padding for operator.

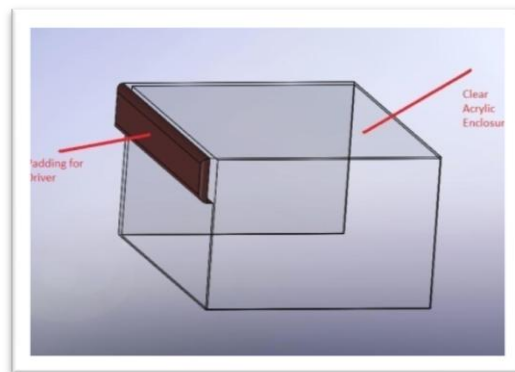


Figure 38 - Solidworks Model of Acrylic Enclosure



Figure 39 - Modified Acrylic Enclosure covering the gearing

Along with guard enclosure for the power train, the team also attached large ¼ inch acrylic panels in the front and rear of the system. These were designed mainly to provide extra safety protection from the large swinging action of the aluminum arm. In the event that something were to go wrong with the arm, the acrylic would provide a reasonable barrier and not hinder the operator's viewing of the entire system.



Figure 40 - Acrylic Panel on Front and Rear of A-frame

7.6.2. Lab Safety

In addition to adding permanent safety components to the structure several new lab safety elements were added. 10in. of heavy duty green foam was added to the underside of both ends of the rocking arm. This was to protect the team from the hard force of the rocking arm. Safety labels were added around the structure, some orange warnings stating “Hard hats and safety goggles required,” as well as safety instructions to ensure that a safe procedure was followed. To insure that hard hats were worn at all times during a lab test, 4 hats were hung on either end of the rocking arm and the rocking arm pivot to ensure that they will not be missed when the extensions (oscillation extension and balance end) are added. Caution-cones and caution-tape was purchased and is used to cordon off the area around the rocking arm when it is in motion.



Figure 41 - Safety rules and Setup of Foam on Arm

7.7. Kite Application

7.7.1. Kite Dynamics

This project deals with the transfer of wind power to electrical energy directly through the lifting force generated by the kite tethered to the end of the rocking arm, thus, understanding and effectively using the flight characteristics of the kites is crucial for success. There have been two kites implemented to date at WPI, while several additional designs are being tested or considered for future use. The kites that have been successfully used are both power kites designed by Peter Lynn, a popular kite boarding manufacturer. Power kites, also known as traction kites, consist of a single elliptical plan form airfoil section tethered to a control bar by either two or four lines. The design is famous for its maneuverability and the impressive lift it generates through careful manipulation of the control surface. Because of their high performance flight characteristics, power kites are used for a variety of extreme sports such as kite boarding, but recent projects have led to nautical applications in which large kites are used by large vessels to increase cruising efficiency.

The power kites used by the MQP are complete kite boarding rigs tethered by four lines. The larger of the two, known as the Guerilla, uses a 10m^2 airfoil section, while the smaller kite, generally used for experiments that do not require the massive lifting performance of the Guerilla, sports a more conservative 6m^2 lifting surface. The general configuration of both kites is shown in the following figure:

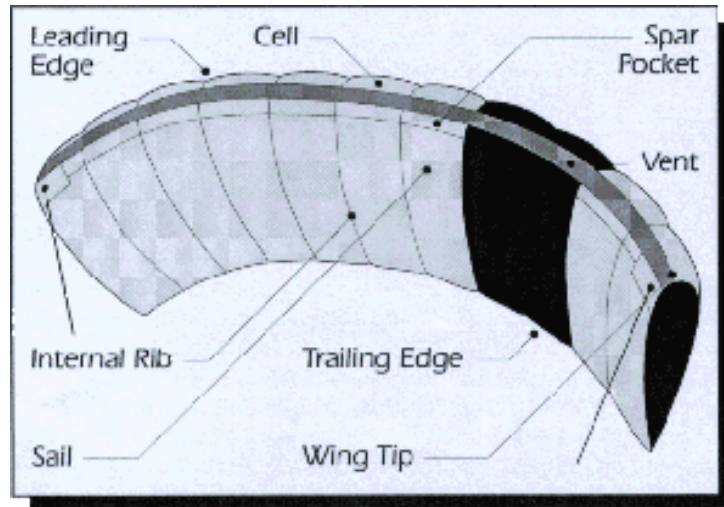


Figure 42 - Diagram of Typical KiteBoarding Kite (AirBorn Kites, 2005)

The kites are tethered to the rocking arm by a line connected to each wingtip on the leading edge as well as a similar pair of lines attached to the trailing edge of the sail. The leading edge tethers support the majority of the lift force and are anchored directly to the rocker arm while the trailing edge lines are attached to the control bar and are responsible for manipulating the control surface and maneuvering the kite on both the vertical and horizontal axis. As far as this project is concerned, it is the vertical maneuvers that are most important considering how the desired oscillatory rocking motion of the arm is achieved through powering and depowering the kite. These maneuvers are achieved through manipulating the kite's angle of attack, that is, the angle formed by the chord of the airfoil with respect to the airflow produced by the wind. The following figure depicts how a power kite is flown by manipulating the control bar:

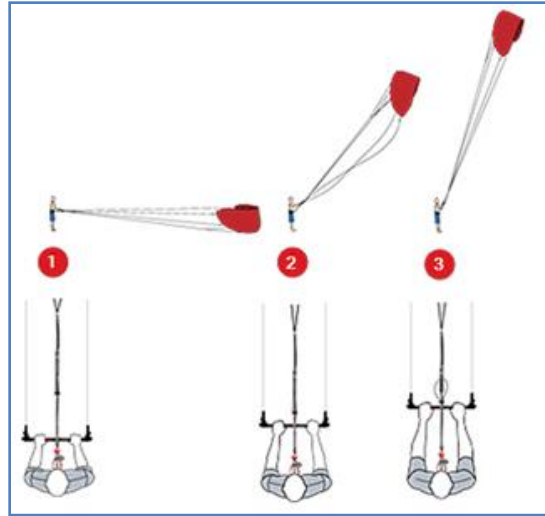


Figure 43 - Illustration of Power/ De-Power Mechanics (PowerKiteShop.com, 2009)

The kite's lift performance is determined by the amount of tension on the trailing edge tethers from user input on the control bar. With the minimum amount of tension, as shown in section one of the figure above, the kite's angle of attack will be near zero and the kite will fly directly overhead with minimum lift, at its 'zenith'. The kite produces lift when the angle of attack is increased by means of pulling back on the control bar (section two in figure). When the control bar is completely moved to the rear of the harness, the angle of attack becomes large enough so that the kite stalls and is effectively de-powered (section three in figure). The following figure illustrates the effect of increasing a generic airfoil's angle of attack in free stream air flow.

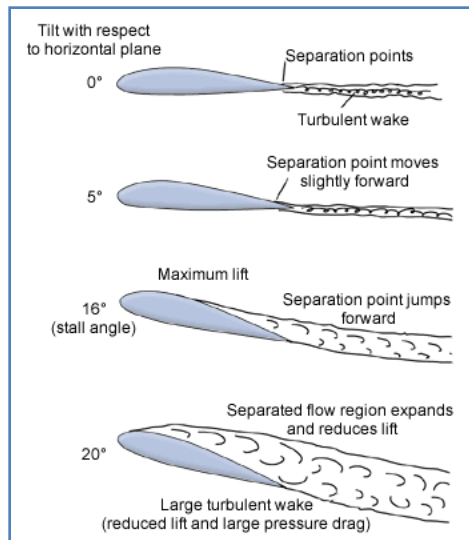


Figure 44 - Angle of Attack with respect to turbulent flow (NASA, 2009)

The primary disadvantage of using kite boarding power kites is that by design they are very maneuverable, and, unfortunately, the kite's plane of flight is not restricted to the vertical axis. The ideal flight path of kite would place the kite directly in line with the rocking arm during its power/ de-power cycle; however, it is a natural tendency for the kite to laterally oscillate in a figure-eight pattern within a forty five degree cone extending from the control bar. The user controls the lateral motion of the kite by simply rotating the control bar much like the handlebars of a bicycle. The flight path is unstable without user input, and if left unattended, the lateral oscillations usually grow in magnitude until the kite crashes. In order to maintain an extended, controlled flight, the group had to improve and implement a custom mount for the kite that would control its flight on both lateral and vertical axis.

7.7.2. Sled Kites

In addition to the power kites, the MQP team has been experimenting with sled kites, a design which involves several features that result in flight characteristics that may prove to be more suitable for project requirements. Sled kites use a parafoil airfoil as well as multiple ram air

pockets in order to generate high lift and directional stability. The beauty of the design, as it pertains to the MQP, is that the kite is attached to the rocker arm by a single tether and thus is free to fly in the direction of the wind without the oscillatory effects that the power kites suffer from.



Figure 45 - Typical Sled Kite (Wind Power Sports, 2007)

8. Testing Methodology

In order to simulate the entire kite demonstrator, all of the structure and subcomponents were tested in the lab. The primary goals of lab testing were:

- Make sure each piece of equipment used for data collection works properly
- Accurately measure 4 variables: torque, force of kite, angle of arm and RPM of shafts
- Compare measured values with theoretical values of 4 variables
- Optimizing gear train setup for power production (engage second power system)
- Look at load/non-load and its effect on the generator
- Insure proper precautions were taken to provide a safe environment for members of team

Each one of the team's goals involved recreating the same conditions as a field test in the lab. This includes trying to create the same forces of the kite that would be tested in the field in order to make accurate hypothesis about what we could expect to see from the wind boarding kite. All of the testing done with the demonstrator took place in the Higgins Fluids lab and loading dock.

Each test was executed in a precise manner. First, safety precautions were taken with the team that included putting on hard-hats, setting up cones and creating a safe area to work in. Second, the demonstrator system was moved to a safe location to give enough overhead clearance for the rocking arm's full range of motion. Third, the front oscillation section and the back sections were attached to the front and rear of the demonstrator, respectively. This included attaching both the first and second power systems (simply attaching chain and/or steel cable to each flat spring mechanism). Fourth, a rope was attached to the front end of the arm and run through a system of pulleys. This is to simulate the force of the kite. A person pulls the rope

downward to pull the front arm upward. The kite is expected to pull upward at up to 200 pounds, therefore, a person's weight would be a good substitute for this application. Finally, each piece of instrumentation was checked for wiring and functionality to the DAQ board.

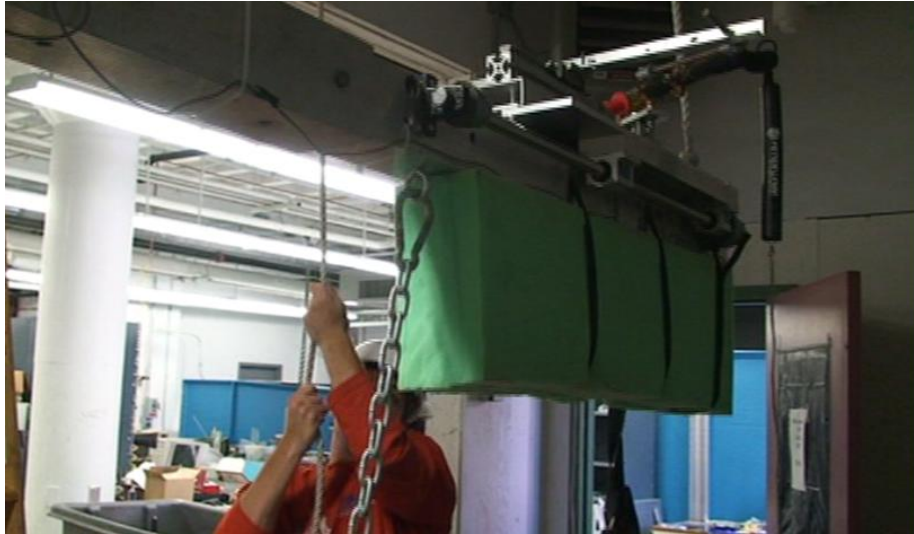


Figure 46 - Testing in Lab with all chains and foam attached to ends of arm

After the entire demonstrator was ready, the team ran a series of tests. Each test was recorded in 2-3 cycles. Each cycle included a pull upward to maximum height and a release of the weight, allowing the natural tension of the second power system to gently bring the arm down to its lowest position. For each test, the weight was kept relatively constant (same person hanging on the rope). Also, the team attached and detached a battery bank to the generator to supply a load on the system. The tests were recorded in LabVIEW and then output to an Excel file where the data could be analyzed.

9. Results

9.1. Lab Testing

Using data collected from lab testing, the kite power system was analyzed. The recorded measurements from each of the four instruments were tabulated in excel and then graphed versus time as shown in Figure 46. Using those measurements we were able to calculate the instantaneous power produced at the flywheel shaft as well as the pivot of the rocking arm. This is shown in Figure 47.

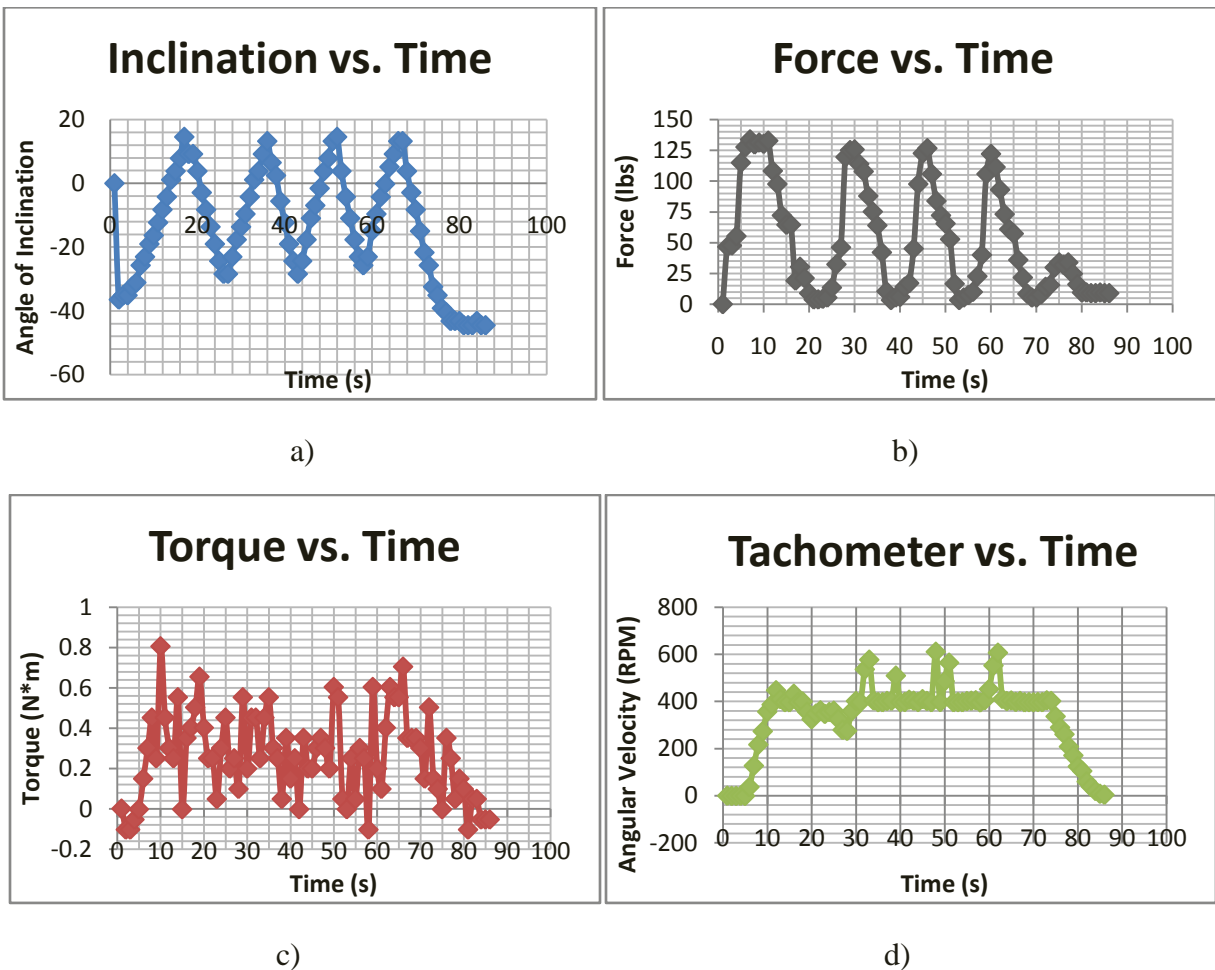


Figure 47 - Instrumentation Curves vs. Time; a) Rocking Arm Inclination; b) Force on Arm; c) Torque on Flywheel Shaft; d) Flywheel Shaft RPM

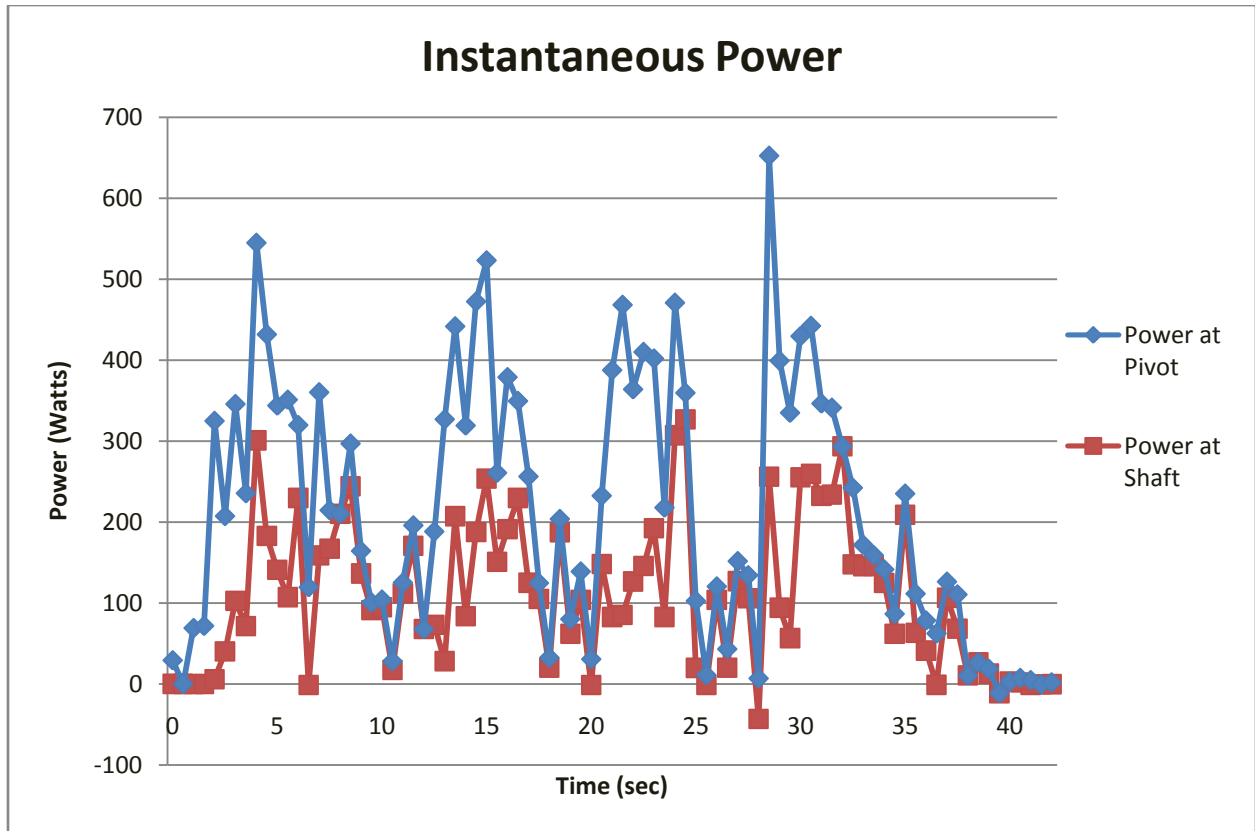


Figure 48 Comparison of Instantaneous Power at Rocking Arm Pivot and Flywheel Shaft

The graphs show a good correlation between the experimental and theoretical values for the various parameters of the kite power system. The expected value of torque at the flywheel shaft was calculated to be approximately 1.05 N*m when the force of the kite on the rocking arm was 200lbs, as discussed in Section 7.2.2. Shown in Figure 46, when the force on the rocking arm was 140lbs (weight of person), the torque meter read about 0.8 N*m. This value matches the theoretical value.

The instantaneous power calculated at the pivot of the rocking arm and at the flywheel shaft is graphed in Figure 46. As expected, the power at the pivot is higher than at the shaft because of mechanical inefficiencies through the gear train and pulley system. From this graph, we can conclude that the mechanical efficiency of the system is highest when the power output is low. This occurs during the kite's descent, when the force on the kite arm is at a minimum and

the inclination of the arm is decreasing towards its minimum. The system is inefficient during the kite's ascent, when the system is powering. This occurs when the force on the kite arm is at its maximum and when the inclination of the arm has reached its minimum and begins to increase again.

There are two additional things to note about the power output. The first is the effectiveness of the secondary power system. On the inclination graph, any point where the slope is negative is where the secondary power system is engaged. The linear slope indicates that the arm is coming down with very controlled motion and not falling to the ground. More importantly, the second system makes up between 55-58% of the power produced by the system, inferring that it effectively more than doubles the amount of power that would occur without it. This was found by taking a sum of the entire power produced and dividing it by the sum of the power produced during the intervals where only the secondary power system is engaged. The second observation worth noting is the efficiency of the drive train with respect to the arm's expected mechanical power output. Through calculations in excel, the data shows that there is only a 25-30% power loss through the friction of the gearing and other mechanical inefficiencies.

Theoretical values of the angular velocity of the flywheel shaft were calculated and compared to the experimental data collected in the lab. The equation used was based on gear ratios and was a function of the angular velocity of the rocking arm:

$$\omega_{shaft} = \frac{R_c}{R_G} * \frac{R_{G2}}{R_{FG}} * \frac{R_{G4}}{R_{G3}} * \omega_{arm}$$

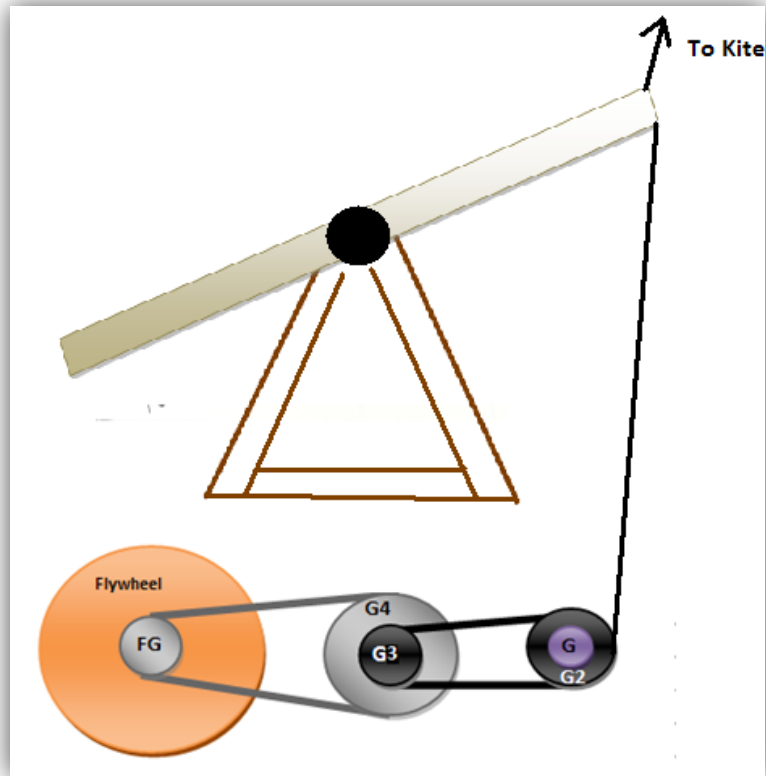


Figure 49 - Diagram of Angular Velocity to Gear Ratio of Drive Train

While comparing the theoretical values of the angular velocity of the flywheel shaft with the recorded measurements from the tachometer, we noticed a slight offset. The residuals of the data, illustrated in Figure 49, show that there was up to a 25% difference between the recorded data to the theoretical predictions. A portion of this could account for various lab errors caused by the imprecision in the mechanical system, such as intense vibration of the gear train that could cause the magnetic pickup to move. However, it was decided that the tachometer also needed to be recalibrated. There was some variation in the tachometer's readings, suggesting that the future MQP team needs to recalibrate the tachometer effectively.

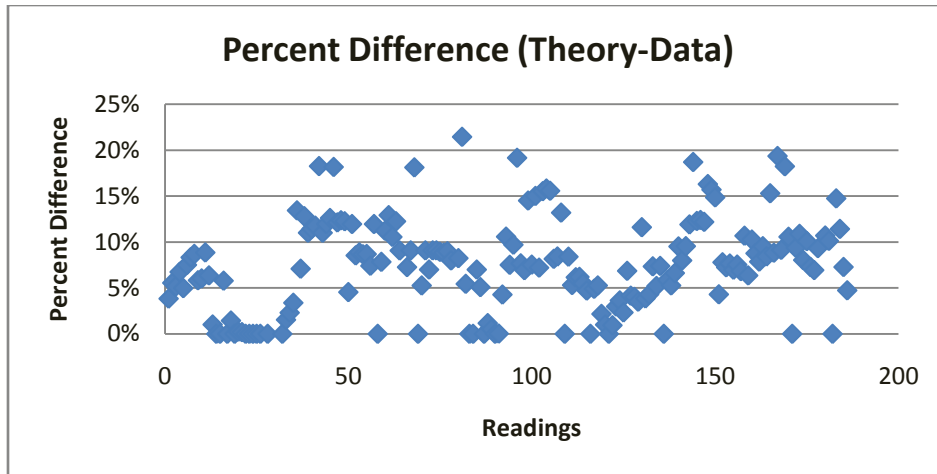


Figure 50 - Percent Difference Data, Expected to Actual

Lastly, an important part of kite power system was storing the power produced. The generator was attached to a battery bank with the intent of capturing the mechanical energy of the system. With the battery bank attached, the generator put more of a torque loading on the shafts to produce power. However, when this was tested in the lab, there was no change in torque or power produced, indicating that, with the connection to the battery banks, the system could not create a high enough voltage to charge them. The system needed to produce at least 26 volts or more through the generator but, at maximum force, the system was only found to produce 15-20 volts. These values were determined by checking the voltage on the generator and the battery bank with a voltmeter.

9.2. Field Testing

While the team worked hard to reproduce realistic environmental conditions in the lab during testing, there is no real substitute for field testing in order to examine the behavior of the kite power system when exposed to the many additional variables in the real world. Throughout the course of the year, the team made several trips to a field location in order to test and evaluate the performance of the kites in various configurations. During the testing, we learned how to assemble and fly the power kites and, in doing so, gained knowledge of how the kites would operate when implemented on the A-frame power system. For safety, we attached the harness to the trailer hitch on Professor Olinger's Ford F-150 truck and operated the control handle without having to withstand the lifting force of the kites. We were also able to experiment with a sled kite and evaluate any potential benefit that would come from transitioning away from using power kites. The sled kite proved to be much more stable than the power kites in all types of wind conditions, but it was too small to compare the lifting performance between the two designs. We attempted to attach trailing edge lines to the sled kite in order to power and de-power the lifting surface in a similar fashion as the power kites, but the small sled kite was unable to fly properly with the added weight of the lines and we experienced tangling problems that prevented us from finding any positive results. Professor Olinger ordered a larger sled kite for testing, but it arrived too late in the year for us to test it in the field. The team hoped to move the entire structure into the field for testing during the spring months to evaluate the performance of the whole system under real world conditions, but, unfortunately, the weather and scheduling never cooperated. Field testing will undoubtedly be a priority as the project progresses in the following semesters.

10. Conclusions

By the end of the project, we were able to prove the value of the kite power concept through lab testing. We were able to successfully build and implement a real-time data collection system measuring four mechanical variables. The data collected can be used to analyze performance and optimize power production. By finding the instantaneous mechanical power of the system, we were able to see how our system operates effectively. Building a secondary power system proved indispensable in optimizing power production, and with the empirical data presented, it was clear how much more energy is now being transferred through the system. The newer oscillation control, although not tested in the field, will add more structural integrity to the rigorous forces that a kite would produce. Although time constraints prevented us from testing the entire demonstrator and data collection in the field, the lab tests conducted were promising in terms of accurately demonstrating the kite force on the arm. Furthermore, the demonstrator was improved for structural integrity for future use.

Overall, the kite system was shown to output electrical power. With the current global state of energy, it is a substantial highlight that we were able to establish the validity of a functional prototype for harnessing a sustainable, clean, and cheap energy. We anticipate that future work in this area will yield excellent results.

10.1. Overall Results

- Developed a working data collection system, effectively measuring:
 - Torque, Kite Force, Angular Velocity, Inclination
 - Instantaneous Power
- Designed subcomponents
 - Secondary Power system
 - Oscillation Control
- Optimized system for better power output
- Extensive lab testing of all components and subcomponents
- Gained comprehensive data on power and effectiveness of mechanical power
- Proved that kite power is a feasible and effective energy technology

11. Future Work

Despite the promising results made by the project, there are still a lot of opportunities left to develop and study the concept of kite power. In the future, one of the primary goals should be to effectively test the kite power demonstrator in the field. This testing should look at three primary areas: field data of the system, autonomous control, and usage of different kite concepts. First, lab tests could only predict the behavior of the system to a certain point. With more field data, the system's validity in terms of power production would be solidified with the comparison to lab testing. Second, more testing of the operator control of the oscillation system is needed. There was an operator chair and rope pulley system installed for this purpose by Professor Olinger. Also, the actual motion of the kite is still somewhat unpredictable, as it depends on immediate weather conditions. Testing in this specific area would be beneficial in terms of being able to gage the real kite's motion as well as making mechanical changes to the system in terms of better control of the kite's movement. This would further the advancement of autonomous control of the kite. Third, different types of kites should be further researched to find the best suitable way of producing kite power, no matter the outdoor conditions.

An immediate goal would be to optimize the charging system and generator's effectiveness. The load of the generator was found to be ineffective, and due to time constraints, the team was unable to create a charge through the current generator setup. Possibly, a better way to store the electrical energy could be researched and designed, using the data of the instrument system to optimize power production.

The system as a whole still needs to be studied in terms of longevity and power optimization. The wooden frame of the system may need to be replaced for longer term usage

(especially in the field). Also, improving on the accuracy of the data collection system would help in terms of finding inefficiencies in the system.

Once a fully functional system is developed, more work can be done to improve the structure and verify the concept in an actual working environment. An ideal location for this work would be WPI's project center in Namibia, Africa. Namibia is in great need of the low-cost, clean electricity this system is designed to generate. The WPI project center focuses largely on sustainable development and would be well suited to sponsor the installation and operation of a kite power system. These are just some of the opportunities for continuing the work done by this project.

12. Reference List

- AirBorn Kites. (2005). *AirBorn Kites Gallery*. Retrieved 1 20, 2009, from AirBorn Kites.com: <http://www.airbornkites.co.uk/catalogue/kites/powerkites/powerkites.gif>
- Blouin, M., Isabella, B., & Rodden, J. (2007). *Wind Power from Kites*. MQP Project, Worcester Polytechnic Institute, Department of Aerospace Engineering, Worcester.
- Buckley, R. e. (2008). *Design of a One Kilowatt Scale Kite Power System*. MQP Project #DJO-0308, Worcester Polytechnic Institute, Department of Aerospace Engineering, Worcester.
- Goela, J. (1983). *Project Report II on Wind Energy Conservation Through Kites*. DST.
- Goela, J. (1979). *Wind Power Through Kites*. Mech Engg.
- Kite Gen. (2008). *Kite Gen Illustration*. Retrieved January 3, 2009, from Kite Gen: <http://www.kitegen.com/images/images/illustrationwf.html>
- Loyd, M. (1980). Crosswind Kite Power. *J. Energy* , 4(3), 106-111.
- Martinelli, N. (2006, October 10). *Generating Power From Kites*. Retrieved January 3, 2009, from Wired Magazine Online: <http://www.wired.com/science/discoveries/news/2006/10/71908>
- NASA. (2009). *The Work of Wings*. Retrieved 1 20, 2009, from NASA Aeronautics: <http://virtualskies.arc.nasa.gov/aeronautics/tutorial/wings.html>
- PowerKiteShop.com. (2009). *Cabrina Crossbow - Power/ Depowering of Kite*. Retrieved January 1, 2009, from PowerKiteShop.com: <http://www.powerkiteshop.com/images/productimages/kites/cabrinhacrossbow/cabrinhacrossbowwidsdepower.jpg>
- Wind Power Sports. (2007). *Image Gallery - Sled Kite*. Retrieved 1 20, 2009, from Wind Power Sports: <http://www.windpowersports.com/kites/singe/images/sled/sled-kite.jpg>

13. Appendix

A. Angle Control for the Rocking Arm

In addition to improving the oscillation control mount on the rocking arm, the project team has also developed several designs that would allow the user to set and adjust the maximum angle of motion for the rocking arm. The problem with the oscillation piece in its current configuration is that the pilot can only depower the kite with the control handle; hence, because the system operates under the power of gravity, the mount is inclined to slide to the rear once the rocking arm rises past parallel and prematurely stall the kite. The proposed design to rectify this problem involves a pair of spring loaded plunger clips situated at the opposing ends of the rails that would secure the mount in both its max-power and depower positions. The clips would be connected by a single cable that would slide freely throughout the rocker arm's power stroke until it is arrested at the arm's desired angle. The tension in the cable would release the clips and allow the mount to slide into the desired configuration. For safety, the cable would include a Spring to relieve some of the stress applied to the frame once it is arrested.

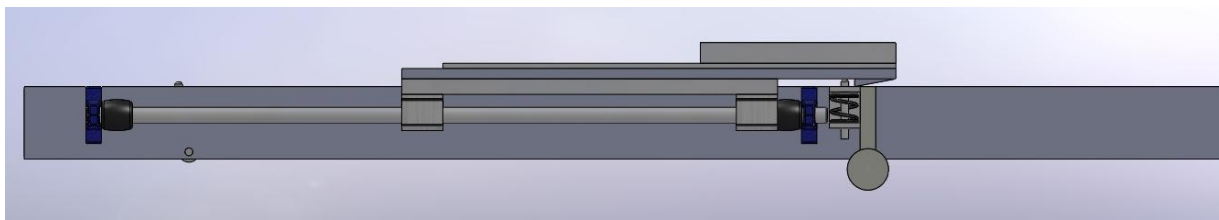


Figure 51 - Oscillation Control Shown with Plunger Clip Assembly

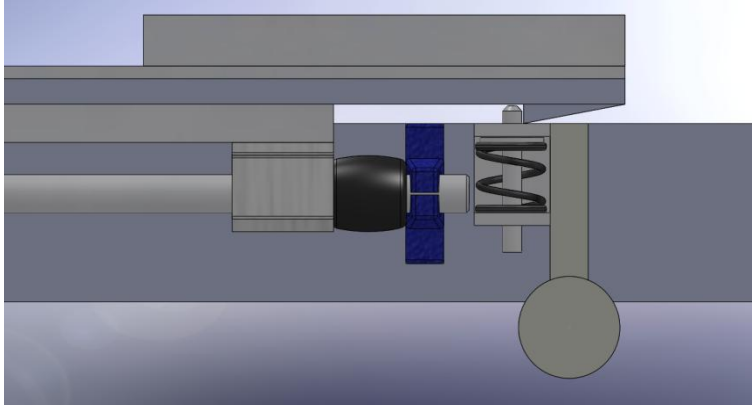


Figure 52 - Detail of rear plunger clip (Note the ramped locking system added to the sliding mount)

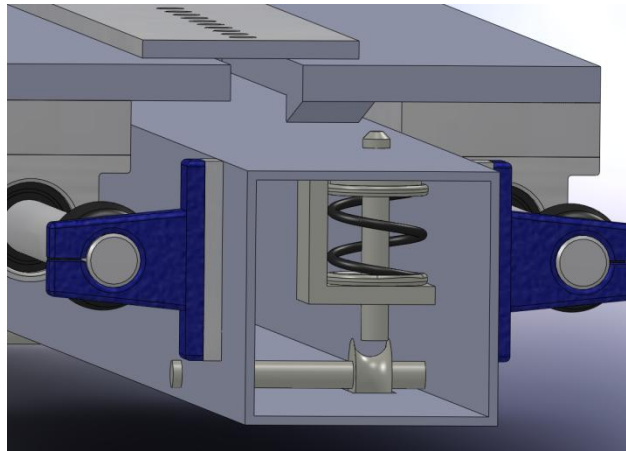


Figure 53 - Detail of Front Plunger Clip